DMD Fast Forward. Published on July 9, 2007 as doi:10.1124/dmd.107.015644

DMD#15644

Prediction of Human Pharmacokinetics Using Physiologically Based Modelling: A Retrospective Analysis of 26 Clinically Tested Drugs

Stefan S. De Buck[1], Vikash K. Sinha, Luca A. Fenu, Marjoleen J. Nijsen, Claire E. Mackie and Ron A. H.J Gilissen

Johnson & Johnson Pharmaceutical Research and Development, Discovery ADME-Tox department, Turnhoutseweg 30, B-2340 Beerse, Belgium [S.S.DB, V.K.S, L.A.F, M.J.N, C.E.M, R.A.H.J.G]

DMD Fast Forward. Published on July 9, 2007 as DOI: 10.1124/dmd.107.015644
This article has not been copyedited and formatted. The final version may differ from this version.

Running title: Prediction of human pharmacokinetics

[1]To whom correspondence should be addressed to: Stefan S. De Buck, Ablynx nv, Technologiepark 4, B-9052 Ghent/Zwijnaarde, Belgium. E-mail address: Stefan.DeBuck@ablynx.com

Text pages: 50
Tables: 8
Figures: 6
References: 38
Words in abstract: 251
Words in introduction: 750
Words in discussion: 1497

ABBREVIATIONS

ACAT, advanced compartmental absorption and transit model; ADME, absorption distribution metabolism excretion; AUC, area under the plasma concentration-time profile; AUMC, area under first moment curve; BCS, Biopharmaceutical Classification Scheme; CL, total body clearance from plasma; CL/F, total body clearance from plasma after oral administration; CL_H, hepatic plasma clearance; $CL_{H,blood}$, hepatic blood clearance; CL_{int}, intrinsic clearance; CL_R, renal clearance from plasma; C_{max}, peak plasma concentration after oral administration; D, dose; F, absolute oral bioavailability; fu_{inc}, unbound fraction in microsomal or hepatocyte incubation; fu_p, unbound fraction in plasma; GFR, glomerular filtration rate; *in vivo* $t_{1/2}$, *in vivo* terminal half-life; $logP_{ow}$, n-octanol:water partition coefficient of the non-ionised species; PBPK, physiologically based pharmacokinetics; PK, pharmacokinetics; P_{tp}, tissue-to-plasma partition coefficient; P_{tpu}, tissue-to-plasma partition coefficient of the unbound drug; Q_h, hepatic blood flow; RA, ratio of albumin concentration found in tissue over plasma; R_B, blood-to-plasma concentration

ratio; SF, scaling factor; SIF, simulated intestinal fluid; Vd/F, apparent volume of distribution after oral administration; Vss, apparent volume of distribution at steady-state

Abstract

The aim of this study was to evaluate different physiologically based modelling strategies for the prediction of human pharmacokinetics. Plasma profiles after intravenous and oral dosing were simulated for 26 clinically tested drugs. Two mechanism-based predictions of human tissue-to-plasma partitioning (P_{tp}) from physicochemical input (Method Vd1) were evaluated for their ability to describe human volume of distribution at steady-state (Vss). This was compared with a strategy that combined predicted and experimentally determined *in vivo* rat P_{tp} data (Method Vd2). Best Vss predictions were obtained using Method Vd2, providing that rat P_{tp}-input was corrected for interspecies differences in plasma protein binding (84% within 2-fold). Vss predictions from physicochemical input alone were poor (32% within 2-fold). Total body clearance (CL) was predicted as the sum of scaled rat renal clearance and hepatic clearance projected from *in vitro* metabolism data. Best CL predictions were obtained by disregarding both blood and microsomal or hepatocyte binding (Method CL2, 74% within 2-fold), while strong bias was seen using both blood and microsomal or hepatocyte binding (Method CL1, 53% within 2-fold). The PBPK model which combined Method Vd2 and CL2 yielded most accurate predictions of *in vivo* terminal half-life (69% within 2-fold). The Gastroplus ACAT model was used to construct an absorption-disposition model and provided accurate predictions of area under the plasma concentration-time profile, oral apparent volume of distribution and maximum plasma concentration after oral dosing, with 74%, 70% and 65% within 2-fold, respectively. This evaluation demonstrates that PBPK models can lead to reasonable predictions of human pharmacokinetics.

DMD Fast Forward. Published on July 9, 2007 as DOI: 10.1124/dmd.107.015644
This article has not been copyedited and formatted. The final version may differ from this version.

In the drug discovery process considerable resources are required to assess the pharmacokinetic (PK) properties of potential drug candidates *in vivo* in animals. In order to optimise the use of such *in vivo* testing, there has been a growing interest in predicting the PK behaviour of drug candidates (Theil et al., 2003; van de Waterbeemd and Gifford, 2003). If sufficiently reliable, such simulations could also help to select the most promising candidates for development and reject those with a low probability of success (van de Waterbeemd and Gifford, 2003).

The majority of the approaches to predict human PK developed to date typically focus on the drug's behaviour in individual processes of absorption, distribution, metabolism and excretion (ADME). The characterization of a drug's PK in a complex biological system is be best described by assembling these processes in one global model. In this context, physiologically based pharmacokinetic models (PBPK) have been developed (Bischoff, 1986). PBPK models map the complex drug transport scheme onto a physiologically realistic compartmental structure (Figure 1). The major structural elements of the PBPK disposition model are derived from the anatomical structure of the organism; therefore, the model structure is predetermined and basically independent of the drug of interest. The PBPK model input parameters include both a drug independent and a drug-specific subset. The first subset comprises data underlying the physiological processes (e.g., blood-flow), while the second subset comprises drug-specific biochemical parameters. The latter consists of the drug's *in vivo* intrinsic clearance (CL_{int}) of each organ involved in its elimination, in addition to estimates of the drug's tissue-to-plasma coefficient (P_{tp}) for each model compartment. Prediction of the rate and extent of absorption can be obtained using semi-physiologically based absorption models, such as the advanced compartmental absorption and transit (ACAT) model (Yu and Amidon, 1999; Agoram et al., 2001). As depicted in Figure 1, the ACAT model may serve as a time-dependent input

function to the disposition model, thereby creating a combined absorption-distribution PBPK model.

Although PBPK models have been widely used in areas such as risk assessment to predict the PK behaviour of toxic chemicals, their application in support of drug discovery and development has remained limited, most probably as a result of their mathematically complexity and the labour intensive drug-specific input data required. However, more recently a variety of *in vitro* based prediction tools have been developed for the estimation of PBPK model input parameters (Theil et al., 2003). Such prediction tools require commonly determined biochemical and physicochemical drug-specific input, and thus allow for the prediction of ADME parameters prior to any *in vivo* experiment. As examples of such prediction tools, mechanistic equations have been developed for the prediction of fraction of oral dose absorbed (Agoram et al., 2001; Willmann et al., 2004), tissue partitioning (P_{tp}) (Poulin and Theil, 2000; Poulin et al., 2001; Rodgers et al., 2005a), apparent volume of distribution at steady-state (Vss) (Poulin and Theil, 2002), and hepatic plasma clearance (CL_H) (Houston and Carlile, 1997; Austin et al., 2002; Ito and Houston, 2004). In a previous study, we also evaluated a variety of physiologically-based prediction tools for the prediction of rat PK (De Buck et al., 2007).

The aim of the present work was to further evaluate these prediction tools for their ability to predict human PK parameters by simulation of full plasma concentration-time profiles after both intravenous and oral administration. Although recent studies have addressed a similar question, the overall prediction accuracy obtained was in the lower range, particularly for predictions of Vss and *in vivo* terminal half-life (*in vivo* $t_{1/2}$) (Parrott et al., 2005b; Jones et al., 2006a). In the present study, a more comprehensive range of approaches towards the prediction of Vss and CL_H was explored; including two mechanism-based Vss predictions from

physicochemical input, as well as approaches that combine the use of both predicted and experimentally determined *in vivo* rat P_{tp}. For each of the approaches tested, the influence of interspecies differences in plasma protein binding on prediction accuracy was investigated. The role of relative drug binding in plasma and *in vitro* drug matrices was also considered with respect to CL_H projection from *in vitro* metabolism data. Whereas the basic tenet of pharmacokinetics states that the unbound drug concentration in the plasma dictates clearance, our previous report in rat using microsomes has suggested that *in vitro* CL_{int} may provide a better estimate of *in vivo* CL_H of total rather than unbound drug (De Buck et al., 2007). To further investigate the effect of relative drug binding, predictions of human CL_H were performed each time under two variations, either by incorporation or disregarding such binding factors. Methods to predict Vss and CL were combined to predict *in vivo* $t_{1/2}$ and the ACAT model was tested for its ability to predict the area under the oral concentration-time profile (AUC), the oral apparent volume of distribution (Vd/F) and peak plasma concentration (C_{max})**.** To determine whether a successful prediction in rat correlates with a successful prediction in human, the accuracy of each method was assessed within both species.

DMD Fast Forward. Published on July 9, 2007 as DOI: 10.1124/dmd.107.015644
This article has not been copyedited and formatted. The final version may differ from this version.

Methods

Compounds and Sources of *In vitro* and *In vivo* Parameters. The set of compounds (n=26) included in this analysis were taken from those brought into clinical development at Johnson & Johnson Pharmaceutical Research and Development (Beerse, Belgium). Compounds were selected based on the availability of historical data on the *in vivo* preclinical (rat) and clinical PK, as well as of each of the following experimentally determined biochemical and physicochemical parameters: unbound fraction in plasma (fu_p), unbound fraction in microsomal or hepatocyte incubation (fu_{inc}), basic and acidic dissociation constants (pKa), n-octanol:water partition coefficient of the non-ionised species ($logP_{ow}$), aqueous solubility at defined pH conditions or solubility in simulated intestinal fluid (SIF), *in vitro* CL_{int} determined in hepatic microsomes or hepatocyte suspension cultures, and the blood-to-plasma concentration ratio (R_B). Summaries of the available *in vitro* and *in vivo* PK data are shown in Tables I and II, respectively.

The 26 compounds in the data set cover a broad range of small molecules from a variety of discovery programs. The majority of compounds (n=19) were moderate-to-strong bases (pKa of protonated base >7.0), three were neutral or weakly ionised at physiological pH (weak base). The remaining compounds were one weak acid, one strong acid, and two were zwitterions. The lipophilicity ($logP_{ow}$) ranged between 1.11 and 5.5, and fu_p ranged from 0.001 to 0.867. Aqueous solubility was highly variable with values at physiological pH ranging from 0.003 mg/ml to 74 mg/ml. Vss in humans varied from limited (30 L) to widespread (>1000 L). In the rat, major elimination pathways included hepatic metabolism, renal excretion or a combination of these. In humans, total body clearance from plasma (CL) varied from less than 10% of hepatic blood flow (Q_h) to more than 70% of Q_h.

DMD Fast Forward. Published on July 9, 2007 as DOI: 10.1124/dmd.107.015644
This article has not been copyedited and formatted. The final version may differ from this version.

Model Structure. The Gastroplus 5.1.0 generic PBPK model and its built-in mass balance differential equations were used for all simulations (Simulations Plus Inc., Lancaster, CA, USA). Briefly, the model (Figure 1) was composed of 14 tissue compartments, including lung, spleen, liver, gut, adipose tissue, muscle, heart, brain, kidney, skin, testes, red marrow, yellow marrow and rest of the body, which were linked by the venous and arterial blood circulation. It was assumed that drug distributes instantaneously and homogenously within each tissue compartment and uptake of drug within each tissue compartment was limited by the blood flow (perfusion rate-limited uptake). The default Gastroplus settings of all physiological data used in the rat and human PBPK models are summarized in Table III. The methods used for estimating the PBPK model input data on CL_H, renal plasma clearance (CL_R), P_{tp} values, and absorption rate are described below.

Prediction of Human and Rat P_{tp} and Vss: Method Vd1. Predicted values of rat and human P_{tp} for each tissue compartment of Figure 1 were obtained from drug-specific physicochemical parameters using the following mechanistic tissue composition-based equation developed by Poulin and coworkers (Poulin and Theil, 2002):

$$P_{tp} = \frac{[P \bullet (V_{NLT} + 0.3 \bullet V_{PHT}) + (V_{WT} + 0.7 \bullet V_{PHT})] \bullet fu_p}{[P \bullet (V_{NLp} + 0.3 \bullet V_{PHp}) + (V_{Wp} + 0.7 \bullet V_{PHp})] \bullet fu_t} \qquad (1)$$

where P is the anti-logged value of $logP_{ow}$ for a non-adipose tissue or is the vegetable oil:buffer partition coefficient for both the ionised and non-ionised species at pH 7.4 (D_{vow}) for adipose tissue. D_{vow} was calculated from $logP_{ow}$ using the Henderson-Hasselbalch equations and the following relationship: $\log P_{vow} = 1.115 \bullet \log P_{ow} - 1.35$ (Leo et al., 1971). V is the fractional tissue volume content of neutral lipids

DMD Fast Forward. Published on July 9, 2007 as DOI: 10.1124/dmd.107.015644
This article has not been copyedited and formatted. The final version may differ from this version.

(NL), phospholipids (PH) or water (W) in tissue (T) and plasma (p). The physiological data on human and rat values used for V_{NLT}, V_{NLp}, V_{PHT}, V_{PHp}, V_{WT}, V_{Wp} have been described in the literature (Poulin and Theil, 2002). The fraction unbound in tissue (fu_t) in equation 1 was estimated as follows:

$$fu_t = 1 / (1+(((1 – fu_p) / fu_p) \bullet RA)) \qquad (2)$$

where RA is the ratio of albumin concentration found in tissue over plasma. For lipophilic and highly protein bound compounds, it has been assumed that for adipose tissue RA equals 0.15, whereas for non-adipose tissue RA equal 0.5 (Ellmerer et al., 2000; Poulin and Theil, 2002).

Finally, rat and human Vss was calculated by Gastroplus software according to the equation of Sawada et al. in which Vss equals the plasma volume in addition to the sum of each P_{tp} multiplied by its respective tissue volume (Sawada et al., 1984).

Prediction of Human and Rat P_{tp} and Vss: Method Vd2. For rat P_{tp} and Vss, experimental rat P_{tp} values were determined under *in vivo* conditions (single oral or intravenous dose) as the ratio of the AUC calculated over a minimum of five time points, assuming pseudo-equilibrium. All experimentally determined *in vivo* rat P_{tp} values used within this study are summarized in Table II. In instances where the *in vivo* P_{tp} was not available for a compound, the value for that tissue compartment (Figure 1) was predicted using the tissue composition-based equation as described by Rodgers et al. (Rodgers et al., 2005a). Briefly, for strong bases (pKa>7.0), P_{tp} of unbound drug (P_{tpu}) was calculated using equation 3:

$$P_{tpu} = \frac{P_{tp}}{fu_p} = \left[\begin{array}{l} V_{EW} + \frac{1 + 10^{\,pKa-7.0}}{1 + 10^{\,pKa-7.4}} \bullet V_{IW} \\ + \frac{K_a \bullet [AP]_t \bullet 10^{\,pKa-7.0}}{1 + 10^{\,pKa-7.4}} \\ + \frac{P_{vow} \bullet V_{NL} + ((0.3 \bullet P_{vow} + 0.7) \bullet V_{NP}))}{1 + 10^{\,pKa-7.4}} \end{array} \right] \qquad (3)$$

DMD Fast Forward. Published on July 9, 2007 as DOI: 10.1124/dmd.107.015644
This article has not been copyedited and formatted. The final version may differ from this version.

where V is the fractional tissue volume of neutral lipids (NL), neutral phospholipids (NP), extracellular water (EW) and intracellular water (IW), $[AP]_t$ is the concentration of acidic phospholipids in tissue, all physiological data on V_{EW}, V_{IW}, V_{NL}, V_{NP} and $[AP]_t$ for both adipose and non-adipose tissue have been described in the literature (Rodgers et al., 2005a), pKa represents the dissociation constant of the protonated base, P_{vow} the anti-logged value of $logP_{vow}$ (calculated from P_{ow} as described above), K_a is the association constant of the compound with the acidic phospholipids, and was calculated from equation 4:

$$K_{a,BC} = \left[P_{tpu,BC} - \frac{1 + 10^{pKa-7.22}}{1 + 10^{pKa-7.4}} \bullet V_{IW} - \frac{P_{vow} \bullet V_{NL,BC} + (0.3 \bullet P_{vow} + 0.7) \bullet V_{NP,BC}}{1 + 10^{pKa-7.4}} \right] \bullet \left[\frac{1 + 10^{pKa-7.4}}{[AP]_{BC} \bullet 10^{pKa-7.22}} \right] \quad (4)$$

where $P_{tpu,BC}$ is the P_{tpu} of the red blood cell (BC) and thus equals the erythrocyte-to-plasma concentration ratio (E:P) divided by fu_p. E:P was calculated from the R_B and hematocrit (H), as follows: $E:P = (R_B–(1–H))/H$. For weak bases (pKa<7, JNJ5, JNJ25, JNJ26), acids (JNJ13, JNJ22) and zwitterions (JNJ17, JNJ19) P_{tp} values were predicted using a modification of equation 3, as described by Rodgers et al. (Rodgers and Rowland, 2006). It should be noted that for all compounds, P_{tp} estimates for testes and rest of body compartment were taken from Method Vd1, as the published equations by Rodgers et al. do not allow for prediction of these values.

For human P_{tp} and Vss, all rat P_{tp} values obtained as described in this section were scaled to human with the assumption that the human P_{tpu} is equal to the rat P_{tpu}:

$$\text{Human } P_{tp} = \frac{\text{Human } fu_p \bullet \text{Rat } P_{tp}}{\text{Rat } fu_p} \quad (5)$$

DMD Fast Forward. Published on July 9, 2007 as DOI: 10.1124/dmd.107.015644
This article has not been copyedited and formatted. The final version may differ from this version.

Finally, rat and human Vss were calculated by Gastroplus software as mentioned under Method Vd1.

Prediction of CL_H, CL_R and CL: Method CL1. For metabolically cleared compounds, the liver compartment of the PBPK model was provided with input data on CL_H, which was calculated in three steps:

Firstly, the *in vitro* hepatic CL_{int} (L/h/mg microsomal protein or L/h/10^6 cells) was determined from a typical microsomal or hepatocyte substrate depletion or kinetic assay (Kantharaj et al., 2003), and was scaled to *in vivo* CL_{int} (L/h), accounting for the microsomal recovery or hepatocellularity and liver weight as described by Houston (Houston, 1994):

$$\textit{in vivo}\ CL_{int} = \textit{in vitro}\ CL_{int} \bullet SF \qquad (6)$$

where SF (Scaling Factor) represents the milligrams of microsomal protein or million cells per gram of liver multiplied by the grams of liver weight. A microsomal recovery of 40 mg microsomal protein/g of liver (Pelkonen et al., 1973; Ito and Houston, 2005) was used for both rat and human. A hepatocellularity of 125 and 120 million cells/g of liver was used for rat and human, respectively (Iwatsubo et al., 1996; Iwatsubo et al., 1997). Human and rat standard liver weight was 1400 g (20 g/kg bodyweight) and 11.25 g (45 g/kg bodyweight), respectively (Houston, 1994; Obach et al., 1997). Secondly, the hepatic blood clearance ($CL_{H,blood,}$) was calculated using the commonly used equation of the well-stirred liver model:

$$CL_{H,blood} = \frac{(fu_p/R_B) \bullet Q_h \bullet (\textit{in vivo}\ CL_{int}/fu_{inc})}{Q_h + (\textit{in vivo}\ CL_{int}/fu_{inc}) \bullet (fu_p/R_B)} \qquad (7)$$

where Q_h is the hepatic blood flow (Human, 90 L/h; Rat, 0.828 L/h). Experimental values for fu_p, fu_{inc}, R_B and *in vivo* CL_{int} are presented in Table I. Finally, as

DMD Fast Forward. Published on July 9, 2007 as DOI: 10.1124/dmd.107.015644
This article has not been copyedited and formatted. The final version may differ from this version.

Gastroplus requires input data on CL_H, $CL_{H,blood}$ was converted to CL_H ($CL_H = R_B \bullet CL_{H,blood}$).

For renally cleared compounds, the prediction of human CL_R was obtained using the glomerular filtration rate (GFR) ratio approach as described by Lin (Lin, 1998):

$$\text{Human } CL_{R,\,unbound} = \frac{\text{Rat } CL_{R,\,unbound}}{\text{GFR ratio}} \qquad (8)$$

where rat $CL_{R,\,unbound}$ (L/h/kg) is the CL_R corrected for rat fu_p (CL_R/fu_p) and the GFR ratio between rat and human is 4.8 (Lin, 1998). Predicted CL was calculated as the sum of the predicted CL_H and CL_R.

Prediction of CL_H, CL_R and CL: Method CL2. Our previous study and those by others using *in vitro* metabolism data have suggested that *in vitro* CL_{int} may provide a better estimate of *in vivo* CL_H of total rather than unbound drug (Obach et al., 1997; De Buck et al., 2007). Therefore, CL_H predictions were also assessed using Method CL2 under the assumption that fu_p/R_B and fu_{inc} effectively nullify in the liver model calculation, negating the measurement of either process:

$$CL_{H,blood} = \frac{Q_h \bullet \textit{ in vivo } CL_{int}}{Q_h + \textit{ in vivo } CL_{int}} \qquad (9)$$

$CL_{H,blood}$ was converted to CL_H as described above. The prediction of human CL_R from rat data was identical to Method CL1. Predicted CL was calculated as the sum of the predicted CL_H and CL_R.

Prediction of *In vivo* $t_{1/2}$: Method Vd1/CL1 and Method Vd2/CL2. Prediction of *in vivo* $t_{1/2}$ relies on the prediction of both Vss and CL. Two different approaches were

tested for their ability to predict *in vivo* $t_{1/2}$: Firstly, Method Vd1 was combined with Method CL1 (i.e., Method Vd1/CL1) as this combination predicts CL_H according to the most widely accepted approach towards the use of fu_p/R_B and fu_{inc} (equation 7) (Jones et al., 2006a), and requires minimal data input for prediction of Vss. For comparison, Method Vd2 was combined with Method CL2 (i.e., Method Vd2/CL2) as this combination predicts Vss and CL according to the approach which was also found to provide best results in rat. Predicted values of *in vivo* $t_{1/2}$ were taken from the Gastroplus software interface.

The ACAT Model and Prediction of Oral AUC. Prediction of oral AUC relies on the prediction of both CL and the extent of absorption. CL was predicted using either Method CL1 or Method CL2 as described above. The extent of absorption was predicted using the Gastroplus ACAT model (Yu and Amidon, 1999; Agoram et al., 2001). For all simulations, the ACAT model was provided with experimentally determined data on $logP_{ow}$, pKa, aqueous buffer solubility or solubility in SIF at defined pH, effective human jejunal permeability (P_{eff}) and dose (D) administered (Table I). Apparent permeability (P_{app}) was measured using a typical Caco-2 permeability assay and converted to P_{eff} using the following correlation: $logP_{eff,human} = 0.6532 \bullet logP_{app,caco\text{-}2} - 0.3036$ (Sun et al., 2002). In instances where Caco-2 data was not available (n=4, Table I), *in silico* estimates of human P_{eff} were obtained by the artificial neural network model in ADMETpredictor version 1.3.2 (Simulations Plus Inc., Lancaster, CA, USA). The extent to which paracellular and transcellular routes are utilized in drug transport is influenced by the fraction of ionized and unionized species, which in turn, depends upon the pKa of the drug and the pH of the solution (Ungell et al., 1998). To account for such regional changes in permeability, the Gastroplus built-in "Opt logD-model" was applied (for a detailed description, see

DMD Fast Forward. Published on July 9, 2007 as DOI: 10.1124/dmd.107.015644
This article has not been copyedited and formatted. The final version may differ from this version.

manual of Gastroplus 5.1.0). In brief, the model assumes that the regional absorption rate coefficient for each GI compartment can be calculated as the product of the P_{eff} (jejunal permeability at pH 6.5) and an absorption scale factor (ASF) specific for each GI compartment. An estimate of ASF for each compartment is obtained based on the premise that a linear relationship with a negative slope exists between the deviation of the logD from the neutral logP ($\Delta logD_{pH}$) and the change in the log of the permeability coefficients at the two pH's:

$$ASF_{pH} = C2 \bullet 10^{C1 \bullet \left(\frac{\Delta logD_{pH} - 6.26}{\Delta logD_{6.5} - 6.26}\right)} \qquad (10)$$

where C1 and C2 are two proprietary fitted constants accomplished through a series of many thousands of simulations. The Gastroplus ACAT physiology was "Human-physiological-Fasted". Metabolic first pass extraction was assumed to depend only on CL_H.

Prediction of Vd/F and C_{max} After Oral Dosing. Prediction of both Vd/F and C_{max} rely on the prediction of Vss, CL and the rate and extent of absorption. The rate and extent of absorption were predicted using the ACAT model as described above. Vss and CL were predicted using either Method Vd1/CL1 or Method Vd2/CL2 as described above. Predicted values of C_{max} were taken from the Gastroplus software interface. The predicted Vd/F was calculated from the predicted CL/F multiplied by the predicted *in vivo* $t_{1/2}$/ln2. Predicted CL/F was calculated as D divided by predicted AUC after oral dosing.

Prediction of Plasma Concentrations After Oral Dosing. Predictions of individual plasma concentrations after oral dosing were obtained using the ACAT model (as

described above), which served as a time-dependent input to the disposition model composed of either Method Vd1/CL1 or Method Vd2/CL2 as described above.

Calculation of the *In vivo* Pharmacokinetic Parameters. Noncompartmental analysis was performed using WinNonLin version 4.01 (Pharsight, Mountain View, CA) to calculate CL from the relationship CL= D/AUC, and Vss was determined as Vss= Dose • AUMC/$(AUC)^2$. Absolute oral bioavailability (F) was calculated as the ratio of dose normalized AUC after oral and intravenous administration using the mean of individual AUCs.

Success Criteria. Success of predictions was assessed by the root mean squared prediction error (*rmse*) and the average-fold error (*afe*) as measures of precision and bias, respectively, with equal value to under- and overpredictions:

$$\text{mse} = \frac{1}{N} \sum (\text{Predicted} - \text{Observed})^2 \text{ , } \text{rmse} = \sqrt{\text{mse}} \qquad (11)$$

$$\text{afe} = 10^{\left| \frac{\sum \log \frac{\text{Predicted}}{\text{Observed}}}{N} \right|} \qquad (12)$$

A prediction method with an *afe* ≤2 was considered successful. Predicted PK parameters and plasma concentration-time profiles were deemed accurate if they agree with mean experimental *in vivo* values within a factor of two (Obach, 1999; Poulin and Theil, 2002).

DMD Fast Forward. Published on July 9, 2007 as DOI: 10.1124/dmd.107.015644
This article has not been copyedited and formatted. The final version may differ from this version.

Results

Prediction of Vss. There were 19 compounds that had human intravenous PK data suitable for assessment of Vss predictions. The correlations between observed and predicted human Vss using Method Vd1 and Vd2 are presented in panel A and B of Figure 2, respectively. The parameters for the accuracy of the predictions using Method Vd1 and Vd2 are given in Table IV and V, respectively. The simplest approach (Method Vd1) predicted human Vss within 2-fold of observed for only 6 compounds (32%, Figure 2A). In contrast, Method Vd2 resulted in more accurate predictions with 16 compounds within 2-fold of observed (84%, Figure 2B). Although Method Vd2 showed slight bias towards overprediction, the bias and precision were typically much better than Method Vd1 as indicated by the decreased *afe* and *rmse* values (Table IV and V). Using Method Vd2, the correction for differences in plasma binding between rat and human resulted in better predictions as compared to when binding differences were ignored (Table VI). Ignoring binding differences yielded more bias and a lower precision, but also a decrease in the number of compounds that were within 2-fold error (Table VI). Furthermore, if in Method Vd2 all experimentally determined *in vivo* rat P_{tp} values were substituted by their predicted counterparts, a general decrease in accuracy was observed, irrespective of correction for plasma binding (Table VI).

Vss prediction accuracy was also assessed in rat to test whether a successful prediction approach in rat indicates that prediction in human would be successful. Method Vd2 was the best predictor of rat Vss, with 73% within 2-fold of observed (n=26), respectively (Table VII). As expected, when all experimentally determined *in vivo* rat P_{tp} values were substituted by their predicted counterparts, a general decrease in accuracy of Method Vd2 was observed. The poorest predictor was Method Vd1,

which predicted only 12 compounds out of 26 within 2-fold of observed (42%, Table VII).

Prediction of CL. The accuracy of clearance predictions refers to the total plasma clearance (CL) when intravenous data were available (n=19). The correlations between observed and predicted human CL using Method CL1 are shown in Figure 2C. Method CL1, which included both blood and microsomal or hepatocyte binding, yielded several underpredictions of CL and only 10 compounds were predicted within 2-fold of mean observed values (53%, Table IV). As a result, a strong bias (*afe*) and poor precision (*rmse*) were observed (Table IV). Despite the overall poor accuracy of the method, prediction of the renal component, i.e., $CL_{R,}$ was found to be accurate. CL_R predictions (n=4) were 6.4 L/h, 18 L/h, 0.74 L/h and 19 L/h for JNJ4, JNJ12, JNJ19, JNJ20, respectively, and therefore all predictions were within 2-fold of observed (Table IV).

The correlations between observed and predicted human CL using Method CL2 are shown in Figure 2D. This method predicted CL within 2-fold of observed for 14 compounds (74%, Figure 2D). Predictions showed limited bias (*afe*) and *rmse* value was strongly decreased as compared to Method CL1 (Table V). To further substantiate these findings, prediction of CL using both Method CL1 and CL2 was also assessed in rat for all compounds (n=26). Table VII indicates that Method CL2 yielded more accurate predictions in rat as compared to Method CL1. Method CL1 projected rat CL within a 2-fold error for only 9 compounds (35%), whereas Method CL2 projected rat CL within 2-fold error for 22 compounds (85%).

Prediction of *In vivo* $t_{1/2}$. The accuracy of the *in vivo* $t_{1/2}$ predictions refers to the terminal *in vivo* $t_{1/2}$ after intravenous administration when intravenous data were

available (n=19), and to the terminal *in vivo* $t_{1/2}$ after oral dosing when only oral data were available (n=7). Panels A and B of Figure 3 illustrate the correlations between the observed and predicted values of *in vivo* $t_{1/2}$ using Method Vd1/CL1 and Method Vd2/CL2, respectively. Method Vd1/CL1 was a poor predictor of *in vivo* $t_{1/2}$ in this analysis in that only 7 compounds were within 2-fold of observed (27%, Figure 3A), with high bias towards overprediction (*afe*) and poor precision (*rmse*) (Table IV). These results were expected based on the results of the individual Methods Vd1 and CL1. In contrast, Method Vd2/CL2 resulted in more accurate predictions of *in vivo* $t_{1/2}$ with 18 compounds within 2-fold of observed (69%, Figure 3B). More importantly, there was significantly less bias (*afe*) and higher precision (*rmse*) (Table V).

Prediction of AUC and F After Oral Dosing. There were 23 compounds that had human oral PK data for assessment of oral AUC, and 16 compounds had both intravenous and oral PK data for assessment of F. The correlations between the observed and predicted oral AUC and F were obtained using the ACAT model in combination with either Method CL1 or Method CL2 and are presented in panels A and B of Figure 4, respectively. Method CL1 predicted oral AUC within 2-fold of observed for only 8 compounds (35%, Figure 4A), and a strong bias towards overprediction was observed for both oral AUC (Figure 4A) and F (Figure 4A, insert). In contrast, Method CL2 predicted oral AUC within 2-fold of observed for 17 compounds (74%, Figure 4B). Prediction of both oral AUC (Figure 4B) and F (Figure 4B, insert) showed less bias and higher precision as indicated by a decreased *afe* and *rmse* value (Table IV and V), respectively.

DMD Fast Forward. Published on July 9, 2007 as DOI: 10.1124/dmd.107.015644
This article has not been copyedited and formatted. The final version may differ from this version.

Prediction of Vd/F and C_{max} After Oral Dosing. The accuracy of the Vd/F predictions was assessed on all compounds intended for the oral route (n=23). Figure 5 illustrates the correlations between the observed and predicted values of Vd/F using the ACAT model in combination with either Method Vd1/CL1 (Figure 5A) or Method Vd2/CL2 (Figure 5B). Method Vd1/CL1 was a poor predictor of Vd/F in that only 5 predictions were within 2-fold of observed (22%, Figure 5A), with high bias towards overprediction (*afe*) and poor precision (*rmse*) (Table IV). In contrast, Method Vd2/CL2 resulted in more accurate predictions of Vd/F with 16 compounds within 2-fold of observed (70%, Figure 5B). Although this method showed slight bias towards underprediction, the bias and precision were typically much better than Method Vd1/CL1 as indicated by the decreased *afe* and *rmse* values (Table IV and V).

The correlations between the observed and predicted C_{max} using the ACAT model in combination with either Method Vd1/CL1 or Method Vd2/CL2 are presented in panels C and D of Figure 5, respectively. Both methods had similar accuracy to predict C_{max} (Table IV and V).

Prediction Accuracy of Oral Plasma Concentrations. There were 23 compounds that had suitable data for assessment of oral plasma concentrations. The simulated plasma concentration-time profiles using the ACAT model in combination with either Method Vd1/CL1 (full line) or Method Vd2/CL2 (dotted line) are shown in Figure 6, together with the observed data (open squares). In general, Method Vd2/CL2 yielded the best agreement between the mean observed and predicted plasma values, as indicated by the *afe* and *rmse* values (Table VIII).

Discussion

The use of whole body PBPK modelling is becoming more popular within the pharmaceutical industry. This is due to a combination of estimating the PK characteristics of compounds as early as possible, with making efficient and informed selection on which compounds to progress (van de Waterbeemd and Gifford, 2003; Jones et al., 2006a). The development of mechanism-based prediction tools for the assessment of P_{tp} and CL_H based on *in vitro* data has greatly contributed to the early applications of PBPK modelling (Theil et al., 2003). Although these prediction tools show great promise, it has been recognized that inaccurate predictions will occur if the underlying assumptions of the mechanistic equations are not met (Parrott et al., 2005b; Jones et al., 2006a). Therefore, more studies are required to assess how the prediction accuracy as well as the type of data needed will vary depending on the approach, the type of chemistry, and prediction system used. To the best of our knowledge, the current study represents the first attempt to explore how an integrated use of both experimental and predicted data can improve PK predictions using whole body PBPK modelling. A dataset of 26 compounds formed the reference data in our study. It is acknowledged that the number of compounds might be below the optimum to draw general conclusions about the usefulness of the approaches investigated, nevertheless it is still large enough to show some clear trends.

The present evaluation indicates that the type of tissue distribution data used must be carefully considered. The most accurate approach towards prediction of human Vss considered a combined set of predicted and experimental *in vivo* rat P_{tp} data (84% within 2-fold, Method Vd2), whereas predictions based on physicochemical input alone were rather poor (32% within 2-fold, Method Vd1). This finding illustrates that Vss predictions can be improved by considering limited experimental *in vivo* rat P_{tp} data (Table II). Experimental P_{tp} data must however be

DMD Fast Forward. Published on July 9, 2007 as DOI: 10.1124/dmd.107.015644
This article has not been copyedited and formatted. The final version may differ from this version.

carefully selected as Vss is largely determined by P_{tp} of adipose and muscle tissue (Bjorkman, 2002), which were available for most of the compounds (Table II). A second clear trend was that correction of rat P_{tp} data for interspecies differences in plasma protein binding yielded better predictions as compared to when binding differences were ignored (84% versus 53% within 2-fold). This observation was anticipated as in scaling tissue distribution from rat to human, the unbound human P_{tp} values are generally assumed to be identical to those of rat (Sawada et al., 1984). Nevertheless, in case of basic drugs, the accuracy of this assumption remains uncertain as electrostatic interactions with acidic phospholipids have been identified as a major factor controlling tissue distribution (Rodgers et al., 2005b), and an interspecies variability in the acidic phospholipids has been indicated (Rodgers et al., 2005a).

Mechanistic equations to predict tissue distribution from physicochemical input have been developed by Poulin and Theil (Poulin and Theil, 2000; Poulin et al., 2001; Poulin and Theil, 2002), who reported that for a set of 123 drugs, 80% of the predicted Vss were within 2-fold of observed. In the current study, the overall prediction accuracy using these equations was reduced to 42% and 32% within 2-fold of observed for rat and human, respectively. A deceased prediction accuracy of these equations was also observed by others (Parrott et al., 2005a; Jones et al., 2006a). This may be explained by distribution processes that are not covered in these equations, such as active transport or ionic interactions of charged bases with acidic phospholipids of cell membranes. In the Poulin and Theil's equation, ionic interactions are not included and tissue binding is extrapolated from plasma protein binding. We have shown that using this approach tissue binding of bases is prone to underestimation, particularly for strong bases that have low plasma protein binding such as JNJ4, JNJ10 and JNJ20 (De Buck et al., 2007). In this study the Vss of most

compounds was however overpredicted, despite the fact that they were bases (Figure 2A). Although this may be explained by a limitation in membrane permeation, this seems rather unlikely given the overall high permeability of the compounds within our dataset. Another explanation may be a consistent overprediction of P_{tp} values of adipose tissue, which is a major contributor to the total Vss. For example, Vss prediction can be easily biased by the investigator's choice on the RA value for adipose tissue (equation 1 and 2). In this study and those by others, it has been assumed that the RA value for adipose tissue equals 0.15 (Jones et al., 2006a). However, in the original work of Poulin and Theil, the RA value for adipose tissue was assumed to be 0 (Poulin and Theil, 2002). Future work will assess whether an optimisation of the RA value based on the outcome of the prediction in rat may improve prediction accuracy.

The decision of whether to incorporate blood binding (fu_p/R_B) and *in vitro* incubation matrix binding (fu_{inc}) in CL_H predictions remains controversial (Obach, 1999; Riley et al., 2005; De Buck et al., 2007). The inclusion of both unbound fractions has been suggested as the generally acceptable approach. However, our results and those by others demonstrate that in the case of some compound classes, especially basic ones, disregarding all binding values may yield the most accurate predictions (Method CL2, 74% within 2-fold) (Obach, 1997; Obach, 1999; De Buck et al., 2007), whereas inclusion of both correction factors yielded large underpredictions (Method CL1, 53% within 2-fold). It is however acknowledged that underpredictions (Figure 2C) may prevail as the contribution of extrahepatic metabolism and biliary clearance to CL has been neglected, therefore scaled microsomal or hepatocyte data may not always be able to fully project CL. To the best of our knowledge, oxidative microsomal metabolism was the major route of elimination for the compounds within this study. Despite these uncertainties, our

findings obtained in human were in agreement with those obtained in rat, suggesting that an assessment of the prediction accuracy in rat could be used to guide which approach is most likely to succeed. For renally cleared compounds (JNJ4, JNJ12, JNJ19, JNJ20), the empirical GFR approach successfully extrapolated human CL_R from rat data. This is in agreement with previous reports that have achieved good predictions of CL_R using this approach (Lin, 1998; Jones et al., 2006a).

The ability to successfully predict a drug's dosing regimen by predicting human *in vivo* $t_{1/2}$ is of tremendous value in the compound selection process. The most accurate prediction of *in vivo* $t_{1/2}$ was obtained using Method Vd2/CL2 (69% within 2-fold). In contrast, *in vivo* $t_{1/2}$ prediction was strongly biased towards overprediction using a combination of method Vd1 and CL1, most probably as a result of overprediction of Vss and underprediction of CL, respectively (Table IV). These results indicate that accurate predictions of both Vss and CL are critical in the prediction of *in vivo* $t_{1/2}$.

In the prediction of oral AUC both the CL and fraction of oral dose absorbed are important. As expected, the most accurate predictions of AUC were obtained using the most accurate input on CL (Method CL2). For the purpose of this study, intestinal wall metabolism was ignored, yet the prediction of oral absorption parameters was on the whole quiet successful, suggesting that the contribution of intestinal metabolism may be low. It is acknowledged that this represents a shortcoming, and ideally its contribution should be considered. Estimates of fraction of oral dosed absorbed were obtained using the ACAT model and were based on the drug's *in vitro* input on permeability and solubility. Unfortunately, in this dataset there were only two BCS class III compounds (high solubility, and low permeability) for which the limiting effect of permeability could be assessed (JNJ10, JNJ12). For such compounds accurate estimates of permeability are imperative for successful

predictions. In this study, converted Caco-2 permeability data provided accurate predictions, while inaccurate predictions were observed using *in silico* predicted counterparts (data not shown). The vast majority of the compounds were highly permeable and belong to either BCS Class I (high solubility) or BCS Class II (low solubility). For BCS class II compounds, the outcome of simulations may be sensitive to the nature and accuracy of the solubility input. Aqueous solubility data may not reflect actual solubility *in vivo*, resulting in a strong bias towards underprediction of bioavailability (Parrott et al., 2005b; Jones et al., 2006a). For two compounds that were practically insoluble in aqueous media (JNJ21, JNJ24), solubility measurements in SIF were found to provide a good alternative.

Prediction of Vd/F and C_{max} rely on the rate of absorption as well as the methods used for prediction of CL and Vss. The ACAT model may serve as a time-dependent input function of PBPK-disposition models, and thus allows to predict full plasma concentration-time profiles. As expected, the most accurate prediction of Vd/F was obtained using Method Vd2/CL2 (70% within 2-fold), while prediction was strongly biased towards overprediction using Method Vd1/CL1 (21% within 2-fold). In contrast, prediction of C_{max} (65% within 2-fold) was less sensitive to the choice of methods used for prediction of Vss and CL. This may be explained by time dependent prediction errors, which are usually more pronounced on terminal plasma concentrations (Figure 6).

In summary, these results and those by others demonstrate that a generic physiologically based prediction approach can lead to reasonable predictions of human pharmacokinetics (Jones et al., 2006a; Jones et al., 2006b). However, the prediction accuracy may vary depending on the approach and significant mis-predictions can occur when the underlying assumptions of the model or prediction tool are not met. PBPK model validation on each of the key input parameters using *in*

vitro assays in combination with preclinical data remains the recommended strategy for human PBPK modelling.

Acknowledgements

The authors would like to thank the many colleagues at Johnson & Johnson Pharmaceutical Research and Development (Beerse, Belgium), who have generated data used in these analyses, with a special thanks to everybody who currently supports the *in vitro* and in *vivo* pharmacokinetic studies and bioanalytical assays.

References

Agoram B, Woltosz WS and Bolger MB (2001) Predicting the impact of physiological and biochemical processes on oral drug bioavailability. *Adv Drug Deliv Rev* **50 Suppl 1:**S41-67.

Austin RP, Barton P, Cockroft SL, Wenlock MC and Riley RJ (2002) The influence of nonspecific microsomal binding on apparent intrinsic clearance, and its prediction from physicochemical properties. *Drug Metab Dispos* **30:**1497-1503.

Bischoff KB (1986) Physiological pharmacokinetics. *Bull Math Biol* **48:**309-322.

Bjorkman S (2002) Prediction of the volume of distribution of a drug: which tissue-plasma partition coefficients are needed? *J Pharm Pharmacol* **54:**1237-1245.

De Buck SS, Sinha VK, Fenu LA, Gilissen RA, Mackie CE and Nijsen MJ (2007) The prediction of drug metabolism, tissue distribution and bioavailability of 50 structurally diverse compounds in rat using mechanism-based ADME prediction tools. *Drug Metab Dispos*.

Ellmerer M, Schaupp L, Brunner GA, Sendlhofer G, Wutte A, Wach P and Pieber TR (2000) Measurement of interstitial albumin in human skeletal muscle and adipose tissue by open-flow microperfusion. *Am J Physiol Endocrinol Metab* **278:**E352-356.

Giuliano C, Jairaj M, Zafiu CM and Laufer R (2005) Direct determination of unbound intrinsic drug clearance in the microsomal stability assay. *Drug Metab Dispos* **33:**1319-1324.

Houston JB (1994) Utility of in vitro drug metabolism data in predicting in vivo metabolic clearance. *Biochem Pharmacol* **47:**1469-1479.

Houston JB and Carlile DJ (1997) Prediction of hepatic clearance from microsomes, hepatocytes, and liver slices. *Drug Metab Rev* **29:**891-922.

Ito K and Houston JB (2004) Comparison of the use of liver models for predicting drug clearance using in vitro kinetic data from hepatic microsomes and isolated hepatocytes. *Pharm Res* **21:**785-792.

Ito K and Houston JB (2005) Prediction of human drug clearance from in vitro and preclinical data using physiologically based and empirical approaches. *Pharm Res* **22:**103-112.

Iwatsubo T, Hirota N, Ooie T, Suzuki H, Shimada N, Chiba K, Ishizaki T, Green CE, Tyson CA and Sugiyama Y (1997) Prediction of in vivo drug metabolism in the human liver from in vitro metabolism data. *Pharmacol Ther* **73:**147-171.

Iwatsubo T, Hirota N, Ooie T, Suzuki H and Sugiyama Y (1996) Prediction of in vivo drug disposition from in vitro data based on physiological pharmacokinetics. *Biopharm Drug Dispos* **17:**273-310.

Jones HM, Parrott N, Jorga K and Lave T (2006a) A novel strategy for physiologically based predictions of human pharmacokinetics. *Clin Pharmacokinet* **45:**511-542.

Jones HM, Parrott N, Ohlenbusch G and Lave T (2006b) Predicting pharmacokinetic food effects using biorelevant solubility media and physiologically based modelling. *Clin Pharmacokinet* **45:**1213-1226.

Kantharaj E, Tuytelaars A, Proost PE, Ongel Z, Van Assouw HP and Gilissen RA (2003) Simultaneous measurement of drug metabolic stability and identification of metabolites using ion-trap mass spectrometry. *Rapid Commun Mass Spectrom* **17:**2661-2668.

Leo A, Hansch C and Elkins D (1971) Partition coefficients and their uses. *Chem Rev* **71:**525-615.

Lin JH (1998) Applications and limitations of interspecies scaling and in vitro extrapolation in pharmacokinetics. *Drug Metab Dispos* **26:**1202-1212.

Obach RS (1997) Nonspecific binding to microsomes: impact on scale-up of in vitro intrinsic clearance to hepatic clearance as assessed through examination of warfarin, imipramine, and propranolol. *Drug Metab Dispos* **25:**1359-1369.

Obach RS (1999) Prediction of human clearance of twenty-nine drugs from hepatic microsomal intrinsic clearance data: An examination of in vitro half-life approach and nonspecific binding to microsomes. *Drug Metab Dispos* **27:**1350-1359.

Obach RS, Baxter JG, Liston TE, Silber BM, Jones BC, MacIntyre F, Rance DJ and Wastall P (1997) The prediction of human pharmacokinetic parameters from preclinical and in vitro metabolism data. *J Pharmacol Exp Ther* **283:**46-58.

Parrott N, Jones H, Paquereau N and Lave T (2005a) Application of full physiological models for pharmaceutical drug candidate selection and extrapolation of pharmacokinetics to man. *Basic Clin Pharmacol Toxicol* **96:**193-199.

Parrott N, Paquereau N, Coassolo P and Lave T (2005b) An evaluation of the utility of physiologically based models of pharmacokinetics in early drug discovery. *J Pharm Sci* **94:**2327-2343.

Pelkonen O, Kaltiala EH, Larmi TK and Karki NT (1973) Comparison of activities of drug-metabolizing enzymes in human fetal and adult livers. *Clin Pharmacol Ther* **14:**840-846.

Poulin P, Schoenlein K and Theil FP (2001) Prediction of adipose tissue: plasma partition coefficients for structurally unrelated drugs. *J Pharm Sci* **90:**436-447.

Poulin P and Theil FP (2000) A priori prediction of tissue:plasma partition coefficients of drugs to facilitate the use of physiologically-based pharmacokinetic models in drug discovery. *J Pharm Sci* **89:**16-35.

Poulin P and Theil FP (2002) Prediction of pharmacokinetics prior to in vivo studies. 1. Mechanism-based prediction of volume of distribution. *J Pharm Sci* **91:**129-156.

Riley RJ, McGinnity DF and Austin RP (2005) A unified model for predicting human hepatic, metabolic clearance from in vitro intrinsic clearance data in hepatocytes and microsomes. *Drug Metab Dispos* **33:**1304-1311.

Rodgers T, Leahy D and Rowland M (2005a) Physiologically based pharmacokinetic modeling 1: predicting the tissue distribution of moderate-to-strong bases. *J Pharm Sci* **94:**1259-1276.

Rodgers T, Leahy D and Rowland M (2005b) Tissue distribution of basic drugs: accounting for enantiomeric, compound and regional differences amongst beta-blocking drugs in rat. *J Pharm Sci* **94:**1237-1248.

Rodgers T and Rowland M (2006) Physiologically based pharmacokinetic modelling 2: predicting the tissue distribution of acids, very weak bases, neutrals and zwitterions. *J Pharm Sci* **95:**1238-1257.

Sawada Y, Hanano M, Sugiyama Y, Harashima H and Iga T (1984) Prediction of the volumes of distribution of basic drugs in humans based on data from animals. *J Pharmacokinet Biopharm* **12:**587-596.

Sun D, Lennernas H, Welage LS, Barnett JL, Landowski CP, Foster D, Fleisher D, Lee KD and Amidon GL (2002) Comparison of human duodenum and Caco-2 gene expression profiles for 12,000 gene sequences tags and correlation with permeability of 26 drugs. *Pharm Res* **19:**1400-1416.

Theil FP, Guentert TW, Haddad S and Poulin P (2003) Utility of physiologically based pharmacokinetic models to drug development and rational drug discovery candidate selection. *Toxicol Lett* **138:**29-49.

Ungell AL, Nylander S, Bergstrand S, Sjoberg A and Lennernas H (1998) Membrane transport of drugs in different regions of the intestinal tract of the rat. *J Pharm Sci* **87:**360-366.

van de Waterbeemd H and Gifford E (2003) ADMET in silico modelling: towards prediction paradise? *Nat Rev Drug Discov* **2:**192-204.

Willmann S, Schmitt W, Keldenich J, Lippert J and Dressman JB (2004) A physiological model for the estimation of the fraction dose absorbed in humans. *J Med Chem* **47:**4022-4031.

Yu LX and Amidon GL (1999) A compartmental absorption and transit model for estimating oral drug absorption. *Int J Pharm* **186:**119-125.

Legends to Figures

Fig. 1. Scheme of the generic disposition PBPK model for simulation of full plasma and tissue concentration-time profiles in rat and human. An overview of all physiological values is given in Table III. Estimation of rate and extent of oral absorption from the gut was obtained using the Advanced Compartmental Absorption and Transit model (ACAT) (Yu and Amidon, 1999; Agoram et al., 2001). For more details on all methods used, refer to the Methods.

Fig. 2. Prediction accuracy for the physiologically based predictions of human volume of distribution at steady-state (Vss) obtained using (**A**) Method Vd1, (**B**) Method Vd2. Prediction accuracy for the physiologically based predictions of human total body clearance from plasma (CL) obtained using (**C**) Method CL1, (**D**) Method CL2. For more details on all methods used, refer to the Methods. Lines signify unity and 2-fold errors between predicted and experimentally determined parameters.

Fig. 3. Prediction accuracy for the physiologically based predictions of human *in vivo* terminal half-life (*in vivo* $t_{1/2}$) obtained using (**A**) Method Vd1/CL1, (**B**) Method Vd2/CL2. For more details on all methods used, refer to the Methods. Lines signify unity and 2-fold errors between predicted and experimentally determined parameters.

Fig. 4. Prediction accuracy for the physiologically based predictions of human area under the plasma concentration-time curve after oral dosing (AUC) and absolute oral bioavailability (F, inserts) obtained using (**A**) the ACAT model and Method CL1, (**B**) the ACAT model and Method CL2. For more details on all methods used, refer to the Methods. Lines signify unity and 2-fold errors between predicted and experimentally determined parameters.

Fig. 5. Prediction accuracy for the physiologically based predictions of the apparent volume of distribution after oral administration (Vd/F) obtained using (**A**) the ACAT model and Method Vd1/CL1, (**B**) the ACAT model and Method Vd2/CL2. Prediction accuracy for the physiologically based predictions of the peak plasma concentration after oral dosing (C_{max}) obtained using (**C**) the ACAT model and Method Vd1/CL1, (**D**) the ACAT model and Method Vd2/CL2. For more details on all methods used, refer to the Methods. Lines signify unity and 2-fold errors between predicted and experimentally determined parameters.

Fig. 6. Predictions of human plasma concentration-time profiles after oral dosing using the ACAT model and either Method Vd1/CL1 (dotted line) or Method Vd2/CL2 (full line) for: (**A**) JNJ1; (**B**) JNJ2; (**C**) JNJ3; (**D**) JNJ4; (**E**) JNJ7; (**F**) JNJ8; (**G**) JNJ9; (**H**) JNJ10; (**I**) JNJ11; (**J**) JNJ12; (**K**) JNJ13; (**L**) JNJ14; (**M**) JNJ15; (**N**) JNJ16; (**O**) JNJ18; (**P**) JNJ19; (**Q**) JNJ20; (**R**) JNJ21; (**S**) JNJ22; (**T**) JNJ23; (**U**) JNJ24; (**V**) JNJ25; (**W**) JNJ26. The observed data is shown in open squares. For more details on all methods used, refer to the Methods.

Table I

In vitro and in silico physicochemical and biochemical properties of the 26 compounds

JNJ #	Generic	Mw	pKa [a]	$LogP_{ow}$ [a]	Species	fu_p [a]	fu_{inc} [b,c,d]	R_B [a]	*in vivo* CL_{int} [e] (ml/min/kg)	Test system [a]	P_{eff} (10^{-4} cm/s) [f,g]	Solubility (mg/ml)
JNJ1	Lorcainide	407	B 9.44	4.16	Rat	0.260	-	1.2	624	RLMic	4.78	265, 214, 192, 2.4, 0.18 in aqueous buffer at pH 2.2, 4.2, 5.9, 7.7 and 9.5, respectively
					Human	0.150	0.45	0.70	31.5	HLMic		
JNJ2	Domperidone	425	B 7.89 B 2.50	3.96	Rat	0.092	-	1.3	178	RLMic	1.88	0.31, 1.5, 0.057, 0.006, 0.001 in aqueous buffer at pH 2.3, 4.2, 6.0, 7.2, 8.0, respectively
					Human	0.061	0.34	0.74	69.3	HLMic		
JNJ3	Nebivolol	405	B 8.40	4.03	Rat	0.015	-	1.2	89.1	RLMic	1.86	0.046, 0.071, 0.91, 0.031, 0.12 in aqueous buffer at pH 1.9, 4.0, 5.4, 6.1, 8.1, respectively
					Human	0.020	0.12 [c]	1.2	11.2	HLMic		
JNJ4	Galantamine	287	B 8.20	1.11	Rat	0.755	-	1.0	20.8	RLMic	5.43	35, 39, 33, 38, 37, 41 in aqueous buffer at pH 2.0, 4.9, 5.2, 6.8, 7.5, 7.7, respectively
					Human	0.822	0.86 [c]	1.2	2.49	HLMic		
JNJ5	Alfentanil	416	B 6.50	2.21	Rat	0.164	-	0.69	416	RLMic	-	-
					Human	0.079	0.97	0.63	190	HLMic		
JNJ6	Sufentanil	386	B 8.10	4.02	Rat	0.069	-	0.74	250	RLMic	-	-
					Human	0.075	0.87	0.74	184	HLMic		
JNJ7	Ketanserin	395	B 7.50	3.30	Rat	0.012	-	0.65	10.0	RLMic	7.14	0.72, 1.30, 16, 15, 11, 0.050, 0.001 in aqueous buffer at pH 1.2, 2.6, 3.1, 3.5, 4.6, 5.7, 8.0, respectively
					Human	0.049	0.32	0.70	31.5	HLMic		
JNJ8	Ritanserin	478	B 8.20 B 2.07	5.20	Rat	0.015	-	0.74	139	RLMic	12.0 [g]	1.4, 0.063, 0.037in aqueous buffer at pH 2.2, 4.1, 6.1, respectively
					Human	0.008	0.45	0.65	4.91	HLMic		
JNJ9	Sabeluzole	415	B 7.60 B 3.40	4.63	Rat	0.016	-	0.84	43.0	RLMic	2.93	

					Human	0.014	0.06	0.82	5.10	HLMic		13, 5.8, 1.3, 3.9, 0.19, 0.01 in aqueous buffer at pH 2.7, 3.3, 4.2, 4.6, 6.0, 6.9, respectively
JNJ10	-	297	B 9.47	4.03	Rat	0.141	-	2.0	312	RLMic	0.321	29, 11, 4.7, 2.9, 0.14, 0.061 in aqueous buffer at pH 3.4, 3.5, 4.5, 7.5, 9.14, 12.8, respectively
					Human	0.115	0.12 [c]	1.4	10.5	HLMic		
JNJ11	Lubeluzole	433	B 7.60 B 4.27	4.88	Rat	0.008	-	0.76	52.0	RLMic	2.79	0.013 in aqueous buffer at pH 6.9
					Human	0.003	0.05 [c]	0.58	3.90	HLMic		
JNJ12	-	296	B 9.88 B 3.00	1.18	Rat	0.820	-	1.5	20.8	RLMic	0.05	20, 20, 20, 7.56, 3.09 in aqueous buffer at pH 1.8, 3.8, 4.3, 7.45, 12.6, respectively
					Human	0.867	0.85 [c]	1.5	0.570	HLMic		
JNJ13	Ridogrel	366	A 4.90 B 3.84	3.54	Rat	0.049	-	0.80	5.10	RLHep	4.73	0.26, 0.02, 0.65, 9.8 in aqueous buffer at pH 2.1, 5.4, 7.0, 8.1, respectively
					Human	0.033	1.0 [d]	0.77	2.20	HLHep		
JNJ14	Laniquidar	584	B 7.90 B 3.30	5.50	Rat	0.002	-	0.79	51.7	RLMic	4.56 [g]	12.4, 0.58, 0.10, 0.064 in aqueous buffer at pH 2.21, 2.78, 3.62, 7.05, respectively
					Human	0.001	0.08	0.62	99.0	HLMic		
JNJ15	Mazapertine	421	B 7.06	3.96	Rat	0.030	-	0.63	623	RLMic	5.70 [g]	80, 43, 0.54, 0.21, 0.22 in aqueous buffer at pH 3.8, 4.7, 6.9, 8.9, 11.5, respectively
					Human	0.011	0.13 [c]	0.52	231	HLMic		
JNJ16	-	686	B 7.20 B 3.10	4.12	Rat	0.036	-	0.78	28.2	RLMic	1.85	13, 1.1, 0.75, 0.04, 0.01 in aqueous buffer at pH 2.2, 3.7, 5.7, 7.5, 8.6, respectively
					Human	0.034	0.08	0.75	20.3	HLMic		
JNJ17	-	558	B 7.26 B 6.18 B 4.00 A 8.28	3.90	Rat	0.028	-	1.0	416	RLMic	-	-
					Human	0.009	0.14 [c]	1.0	231	HLMic		
JNJ18	Risperidone	411	B 8.24 B 3.11	3.04	Rat	0.118	-	0.85	250	RLMic	5.70	40, 4.1, 1.8, 0.25, 0.064 in aqueous buffer at pH 5.4, 6.0, 6.2, 7.5, 8.7, respectively
					Human	0.100	0.34	0.67	7.96	HLMic		
JNJ19	Levocabastine	420	B 9.90 A 3.20	1.75	Rat	0.465	-	1.1	1.25	RLHep	2.10	

					Human	0.453	1.0 [d]	1.2	0.33	HLHep		0.06, 0.05, 0.02, 0.02 in aqueous buffer at pH 2.0, 3.2, 6.0, 8.0, respectively
JNJ20	Norcisapride	313	B 9.10	B 3.00	1.51	Rat	0.650	-	1.5	2.43	RLMic	1.16	80, 92, 93, 74, 41 in aqueous buffer at pH 2.1, 4.8, 6.6, 7.8, 8.0, respectively
						Human	0.625	0.79 [c]	1.6	0.88	HLMic		
JNJ21	-	481	B 7.27		3.55	Rat	0.015	-	1.5	35.6	RLMic	1.96	0.05 in aqueous buffer at pH 1.2, 0.003 in SIF[a] at pH 7.53
						Human	0.012	0.23	1.5	77.0	HLMic		
JNJ22	-	570	A 8.21		4.78	Rat	0.001	-	0.74	156	RLMic	0.751	0.002 and 100 in aqueous buffer at pH 6.5 and 8.7, respectively and 0.249 in SIF[a] at pH 7.5
						Human	0.001	0.90	0.55	116	HLMic		
JNJ23	-	359	B 7.00	B 3.10	3.40	Rat	0.082	-	0.80	208	RLMic	3.41	10.3, 3.9, 0.42, 0.035, 0.002 in aqueous buffer at pH 3.0, 4.2, 5.1, 6.0, 8.1, respectively
						Human	0.016	0.06	0.61	10.2	HLMic		
JNJ24	-	380	B 7.23	B 5.20	5.24	Rat	0.007	-	0.75	371	RLHep	2.00	20, 10.2, 2.19, 0.026 in aqueous buffer at pH 1.4, 4.4, 5.2, 6.0, respectively and 0.005 SIF[a] at pH 7.4
						Human	0.006	1.0 [d]	0.59	8.97	HLHep		
JNJ25	-	660	B 6.80	B 2.86	4.84	Rat	0.015	-	0.70	19.9	RLMic	4.54 [g]	1.6, 2.43, 0.52, 0.02, 0.01 in aqueous buffer at pH 2.1, 4.4, 5.0, 7.0, 9.0, respectively
						Human	0.016	0.05 [c]	0.72	7.28	HLMic		
JNJ26	-	500	B 5.95	B 3.67	4.00	Rat	0.036	-	1.3	24.8	RLHep	2.07	2.3, 0.18, 0.014, 0.005 in aqueous buffer at pH 2.3, 4.5, 5.9, 7.5
						Human	0.023	1.0 [d]	1.5	9.03	HLHep		

[a] A, acid; B, base; R_B, blood-to-plasma partition coefficient; fu_p, fraction unbound in plasma; HLHep, human liver hepatocytes; HLMic, human liver microsomes; $logP_{ow}$, octanol:water partition coefficient; RLHep, rat liver hepatocytes; RLMic, rat liver microsomes; SIF, simulated intestinal fluid

[b] fu_{inc}, experimentally determined unbound fraction in *in vitro* incubation matrix. Experimental values of fu_{inc} in human microsomal protein was determined according to (Giuliano et al., 2005). Rat fu_{inc} was assumed to equal human fu_{inc}

[c] Predicted fu_{inc} value in microsomes according to (Austin et al., 2002)

[d] Hepatocyte incubation performed in protein-free medium (fu_{inc}=1)

[e] *in vivo* CL_{int}, *in vivo* intrinsic clearance calculated using equation 6 as described in the Methods

[f] Permeability measured using a Caco-2 assay and converted to effective human jejunal permeability (P_{eff}) using the reported correlation $logP_{eff,human} = 0.6532 \bullet logP_{app,caco-2} - 0.3036$ (Sun et al., 2002).

[g] *In silico* predicted P_{eff} (ADMETpredictor software version 1.3.2, Simulations Plus Inc., Lancaster, CA, USA)

Table II

Summary of the preclinical (rat) and clinical pharmacokinetic data for the 26 compounds.

JNJ#	Species	D [a] (mg)	Route	CL or CL/F [a] (L/h)	CL_R [a] (L/h)	Vss or Vd/F [a] (L)	*in vivo* $t_{1/2}$ [a] (h)	C_{max} [a] (ng/ml)	AUC [a] (ng.h/ml)	Experimentally determined *in vivo* rat P_{tp} [b]										
										lung	adipose	muscle	liver	spleen	heart	brain	kidney	skin	testes	bone
JNJ1	Human	100	IV	71.6	-	413	5.10	-	1.40E+03	-	-	-	-	-	-	-	-	-	-	-
	Human	100	PO	202	-	1.49E+03	-	60.1	494	-	-	-	-	-	-	-	-	-	-	-
	Rat	2.50	IV	1.55	-	3.92	2.91	-	1.61E+03	19.4	5.27	6.50	0.571	10.3	2.91	1.52	5.68	-	-	-
	Rat	1.88	PO	4.24	-	-	-	-	442	-	-	-	-	-	-	-	-	-	-	-
										-	-	-	-	-	-	-	-	-	-	-
JNJ2	Human	10.0	IV	34.3	-	157	7.59	-	292	-	-	-	-	-	-	-	-	-	-	-
	Human	60.0	PO	232	-	2.54E+03	-	102	259	-	-	-	-	-	-	-	-	-	-	-
	Rat	0.625	IV	1.30	-	1.39	0.871	-	480	10.9	3.21	3.45	13.8	-	3.87	-	22.5	4.35	-	-
	Rat	0.625	PO	6.01	-	-	-	-	104	-	-	-	-	-	-	-	-	-	-	-
										-	-	-	-	-	-	-	-	-	-	-
JNJ3	Human	0.500	IV	80.5	-	1.14E+03	10.40	-	6.20	-	-	-	-	-	-	-	-	-	-	-
	Human	5.00	PO	192	-	2.87E+03	-	2.01	26.1	-	-	-	-	-	-	-	-	-	-	-
	Rat	0.313	IV	0.736	-	1.55	1.37	-	425	99.7	2.67	2.95	14.1	15.6	4.71	3.73	10.6	7.65	5.32	7.87;14.1
	Rat	0.313	PO	0.925	-	-	-	-	338	-	-	-	-	-	-	-	-	-	-	-
										-	-	-	-	-	-	-	-	-	-	-
JNJ4	Human	8.00	IV	17.8	3.93	175	7.40	-	482	-	-	-	-	-	-	-	-	-	-	-
	Human	8.00	PO	18.7	-	200	-	42.6	427	-	-	-	-	-	-	-	-	-	-	-
	Rat	0.625	IV	0.473	0.100	1.30	3.48	-	1.32E+03	4.42	0.476	2.14	2.53	2.92	2.28	1.51	14.5	1.14	1.46	4.79;4.81

	Rat	0.625	PO	0.803	-	-	-	-	778	-	-	-	-	-	-	-	-	-	-	-
										-	-	-	-	-	-	-	-	-	-	-
JNJ5	Human	8.75	IV	21.2	-	28.8	1.37	-	510	-	-	-	-	-	-	-	-	-	-	-
	Human	-	PO	-	-	-	-	-	-	-	-	-	-	-	-	-	-	-	-	-
	Rat	4.00E-02	IV	0.464	-	0.110	0.146	-	86.2	1.11	3.01	0.440	1.43	1.05	0.791	0.181	1.18	0.512	0.481	-
	Rat	-	PO	-	-	-	-	-	-	-	-	-	-	-	-	-	-	-	-	-
										-	-	-	-	-	-	-	-	-	-	-
JNJ6	Human	0.350	IV	49.6	-	128	2.47	-	8.10	-	-	-	-	-	-	-	-	-	-	-
	Human	-	PO	-	-	-	-	-	-	-	-	-	-	-	-	-	-	-	-	-
	Rat	6.25E-04	IV	1.04	-	0.967	1.05	-	0.604	6.18	7.72	1.71	0.370	2.80	1.80	2.08	1.17	-	1.97	-
	Rat	-	PO	-	-	-	-	-	-	-	-	-	-	-	-	-	-	-	-	-
										-	-	-	-	-	-	-	-	-	-	-
JNJ7	Human	10.0	IV	33.9	-	268	14.3	-	298	-	-	-	-	-	-	-	-	-	-	-
	Human	20.0	PO	71.7	-	1.48E+03	-	71.4	279	-	-	-	-	-	-	-	-	-	-	-
	Rat	2.50	IV	5.75E-02	-	0.168	2.00	-	4.35E+04	1.49	0.562	0.284	2.60	0.911	0.354	0.194	1.53	0.463	0.495	0.19;0.18
	Rat	2.50	PO	9.82E-02	-	-	-	-	2.55E+04	-	-	-	-	-	-	-	-	-	-	-
										-	-	-	-	-	-	-	-	-	-	-
JNJ8	Human	5.00	IV	2.14	-	99.0	40.0	-	2.51E+03	-	-	-	-	-	-	-	-	-	-	-
	Human	10.0	PO	2.33	-	134	-	164	4.30E+03	-	-	-	-	-	-	-	-	-	-	-
	Rat	0.625	IV	0.400	-	2.00	2.52	-	1.56E+03	27.8	4.29	3.02	21.8	-	-	10.5	14.1	-	-	-
	Rat	0.625	PO	0.918	-	-	-	-	681	-	-	-	-	-	-	-	-	-	-	-
										-	-	-	-	-	-	-	-	-	-	-
JNJ9	Human	10.0	IV	17.0	-	385	18.9	-	594	-	-	-	-	-	-	-	-	-	-	-
	Human	5.00	PO	22.7	-	621	-	14.5	220	-	-	-	-	-	-	-	-	-	-	-

Rat	0.313	IV	0.538	-	1.46	2.13	-	581	29.2	8.41	0.831	37.7	5.48	2.45	5.37	10.4	2.95	4.62	1.83;7.76
Rat	0.625	PO	1.24	-	-	-	-	506	-	-	-	-	-	-	-	-	-	-	-
									-	-	-	-	-	-	-	-	-	-	-
JNJ10 Human	1.00	IV	149	-	1.33E+03	7.09	-	6.58	-	-	-	-	-	-	-	-	-	-	-
Human	8.00	PO	950	-	9.72E+03	-	0.590	8.42	-	-	-	-	-	-	-	-	-	-	-
Rat	2.50	IV	2.02	-	8.37	2.77	-	1.24E+03	400	-	20.1	150	-	40.2	80.3	80.1	-	75.1	-
Rat	10.0	PO	5.26	-	-	-	-	1.90E+03	-	-	-	-	-	-	-	-	-	-	-
									-	-	-	-	-	-	-	-	-	-	-
JNJ11 Human	10.0	IV	8.46	-	181	17.6	-	1.22E+03	-	-	-	-	-	-	-	-	-	-	-
Human	10.0	PO	13.1	-	333	-	52.6	763	-	-	-	-	-	-	-	-	-	-	-
Rat	0.158	IV	0.375	-	1.06	2.05	-	420	18.1	13.8	2.04	31.7	7.51	3.66	4.13	9.91	4.62	6.32	2.67;11.1
Rat	-	PO	-	-	-	-	-	-	-	-	-	-	-	-	-	-	-	-	-
									-	-	-	-	-	-	-	-	-	-	-
JNJ12 Human	30.0	IV	16.6	9.24	122	8.20	-	196	-	-	-	-	-	-	-	-	-	-	-
Human	30.0	PO	184	-	2.18E+03	-	15.6	163	-	-	-	-	-	-	-	-	-	-	-
Rat	1.25	IV	0.550	0.300	1.77	2.90	-	2.27E+03	7.17	-	1.01	45.9	-	2.81	1.02	10.7	1.03	-	-
Rat	0.625	PO	78.1	-	-	-	-	8.00	-	-	-	-	-	-	-	-	-	-	-
									-	-	-	-	-	-	-	-	-	-	-
JNJ13 Human	100	IV	4.41	-	30.3	7.54	-	2.29E+03	-	-	-	-	-	-	-	-	-	-	-
Human	400	PO	4.61	-	50.2	-	1.71E+04	8.67E+04	-	-	-	-	-	-	-	-	-	-	-
Rat	2.50	IV	3.00E-02	-	0.194	5.10	-	8.33E+04	0.371	-	0.111	1.39	-	0.389	0.178	0.251	-	-	-
Rat	2.50	PO	4.07E-02	-	-	-	-	6.15E+04	-	-	-	-	-	-	-	-	-	-	-
									-	-	-	-	-	-	-	-	-	-	-
JNJ14 Human	50.0	IV	59.4	-	422	10.6	-	882	-	-	-	-	-	-	-	-	-	-	-

Human	200	PO	568	-	8.69E+03	-	187	352	-	-	-	-	-	-	-	-	-	-	-
Rat	4.55	IV	0.697	-	2.24	2.92	-	6.53E+03	38.7	25.5	7.07	16.8	8.44	5.82	2.86	12.0	8.52	3.81	1.83;8.32
Rat	2.50	PO	2.52	-	-	-	-	994	-	-	-	-	-	-	-	-	-	-	-
									-	-	-	-	-	-	-	-	-	-	-
JNJ15 Human	2.80	IV	25.9	-	108	4.60	-	-	-	-	-	-	-	-	-	-	-	-	-
Human	40.0	PO	56.4	-	374	-	-	0.650	-	-	-	-	-	-	-	-	-	-	-
Rat	1.25	IV	0.588	-	0.433	1.94	-	2.13E+03	2.31	8.01	1.49	20.5	1.55	1.52	0.620	7.36	1.12	0.762	-
Rat	7.50	PO	2.96	-	-	-	-	2.54E+03	-	-	-	-	-	-	-	-	-	-	-
									-	-	-	-	-	-	-	-	-	-	-
JNJ16 Human	50.0	IV	36.0	-	717	18.9	-	1.37E+03	-	-	-	-	-	-	-	-	-	-	-
Human	200	PO	68.1	-	1.86E+03	-	220	2.94E+03	-	-	-	-	-	-	-	-	-	-	-
Rat	0.500	IV	0.370	-	1.46	2.92	-	1.35E+03	46.7	-	3.24	35.5	20.9	7.73	0.661	14.1	-	2.35	-
Rat	2.50	PO	0.440	-	-	-	-	5.68E+03	-	-	-	-	-	-	-	-	-	-	-
									-	-	-	-	-	-	-	-	-	-	-
JNJ17 Human	75.0	IV	31.2	-	172	5.14	-	2.45E+03	-	-	-	-	-	-	-	-	-	-	-
Human	-	PO	-	-	-	-	-	-	-	-	-	-	-	-	-	-	-	-	-
Rat	0.500	IV	1.40	-	15.4	6.67	-	357	56.1	15.3	20.5	48.2	50.4	40.1	1.12	92.3	10.1	2.11	-
Rat	2.50	PO	-	-	-	-	-	-	-	-	-	-	-	-	-	-	-	-	-
									-	-	-	-	-	-	-	-	-	-	-
JNJ18 Human	1.00	IV	23.6	0.780	81.0	2.80	-	45.3	-	-	-	-	-	-	-	-	-	-	-
Human	1.00	PO	31.3	-	126	-	7.90	32.0	-	-	-	-	-	-	-	-	-	-	-
Rat	0.313	IV	0.962	-	0.443	0.600	-	325	3.42	-	0.581	12.3	-	0.822	0.233	6.43	-	-	-
Rat	0.313	PO	3.52	-	-	-	-	88.8	-	-	-	-	-	-	-	-	-	-	-
									-	-	-	-	-	-	-	-	-	-	-

JNJ19	Human	0.200	IV	1.82	1.26	82.2	33.0	-	115	-	-	-	-	-	-	-	-	-	-	-
	Human	2.00	PO	1.75	-	83.4	-	23.0	1.14E+03	-	-	-	-	-	-	-	-	-	-	-
	Rat	2.50E-02	IV	4.05E-02	0.013	0.340	6.00	-	617	1.49	0.840	0.883	14.0	1.32	1.19	0.589	8.52	0.978	0.982	0.52;1.56
	Rat	0.625	PO	4.87E-02	-	-	-	-	1.28E+04	-	-	-	-	-	-	-	-	-	-	-
										-	-	-	-	-	-	-	-	-	-	-
JNJ20	Human	-	IV	-	25.2	-	-	-	-	-	-	-	-	-	-	-	-	-	-	-
	Human	15.0	PO	56.4	-	646	9.00	36.1	266	-	-	-	-	-	-	-	-	-	-	-
	Rat	1.25	IV	0.605	0.350	1.59	2.30	-	2.07E+03	-	-	-	-	-	-	-	-	-	-	-
	Rat	2.50	PO	1.11	-	-	-	-	2.24E+03	-	-	-	-	-	-	-	-	-	-	-
										-	-	-	-	-	-	-	-	-	-	-
JNJ21	Human	-	IV	-	-	-	-	-	-	-	-	-	-	-	-	-	-	-	-	-
	Human	150	PO	773	-	3.04E+03	21.2	39.3	194	-	-	-	-	-	-	-	-	-	-	-
	Rat	0.250	IV	0.410	-	2.68	5.86	-	610	-	-	7.25	23.3	-	6.91	4.35	-	-	-	-
	Rat	1.25	PO	1.10	-	-	-	-	1.14E+03	-	-	-	-	-	-	-	-	-	-	-
										-	-	-	-	-	-	-	-	-	-	-
JNJ22	Human	-	IV	-	-	-	-	-	-	-	-	-	-	-	-	-	-	-	-	-
	Human	300	PO	602	-	687	1.40	301	498	-	-	-	-	-	-	-	-	-	-	-
	Rat	6.25	IV	0.175	-	5.25E-02	1.20	-	3.57E+04	-	-	-	-	-	-	-	-	-	-	-
	Rat	10.0	PO	0.730	-	-	-	-	1.37E+04	-	-	-	-	-	-	-	-	-	-	-
										-	-	-	-	-	-	-	-	-	-	-
JNJ23	Human	-	IV	-	-	-	-	-	-	-	-	-	-	-	-	-	-	-	-	-
	Human	16.0	PO	17.9	-	53.4	3.50	314	894	-	-	-	-	-	-	-	-	-	-	-
	Rat	0.375	IV	0.500	-	0.369	0.545	-	750	2.48	2.53	0.665	8.64	3.35	1.34	1.39	4.03	0.915	1.72	0.69;3.79
	Rat	1.33	PO	1.65	-	-	-	-	803	-	-	-	-	-	-	-	-	-	-	-

									-	-	-	-	-	-	-	-	-	-	-
JNJ24	Human	-	IV	-	-	-	-	-	-	-	-	-	-	-	-	-	-	-	-	-
	Human	80.0	PO	26.5	-	635	26.6	551	3.02E+03	-	-	-	-	-	-	-	-	-	-	-
	Rat	0.625	IV	0.829	-	0.947	2.40	-	754	3.43	3.36	4.36	27.9	2.53	2.65	1.00	4.89	0.936	4.53	0.58;2.54
	Rat	1.25	PO	9.77	-	-	-	-	128	-	-	-	-	-	-	-	-	-	-	-
										-	-	-	-	-	-	-	-	-	-	-
JNJ25	Human	-	IV	-	-	-	-	-	-	-	-	-	-	-	-	-	-	-	-	-
	Human	200	PO	19.9	-	413	22.7	701	1.01E+04	-	-	-	-	-	-	-	-	-	-	-
	Rat	0.625	IV	0.320	-	1.735	4.33	-	1.95E+03	20.6	3.80	2.27	11.7	6.74	4.27	0.663	2.96	1.09	0.666	0.63;2.44
	Rat	1.25	PO	0.373	-	-	-	-	3.35E+03	-	-	-	-	-	-	-	-	-	-	-
										-	-	-	-	-	-	-	-	-	-	-
JNJ26	Human	-	IV	-	-	-	-	-	-	-	-	-	-	-	-	-	-	-	-	-
	Human	20.0	PO	38.8	-	292	9.80	99	516	-	-	-	-	-	-	-	-	-	-	-
	Rat	0.625	IV	0.365	-	0.609	1.47	-	1.71E+03	2.51	20.0	1.20	2.10	1.10	1.70	0.500	2.00	2.51	2.11	2.72;20.0
	Rat	2.50	PO	11.1	-	-	-	-	226	-	-	-	-	-	-	-	-	-	-	-

[a] AUC, area under the plasma concentration-time curve; CL, total body clearance from plasma; CL/F, total body clearance from plasma after oral dosing; C_{max}, peak plasma concentration; *in vivo* $t_{1/2}$, *in vivo* terminal half-life; D, Dose; Vss, volume of distribution at steady-state; Vd/F, apparent volume of distribution during terminal phase after oral dosing

[b] P_{tp}, tissue-to-plasma partition coefficient. Experimental rat P_{tp} values were determined under *in vivo* conditions (single oral or intravenous dose) as the ratio of the AUC calculated over a minimum of five time points, assuming pseudo-equilibrium. Underlined values refer to *in vivo* rat P_{tp} obtained using total radioactivity measurements

Table III

Physiological values for tissue volumes and blood flows in rat and human [a]

	Rat		Human	
Tissue	Blood flow (ml/min)	Volume (ml)	Blood flow (L/min)	Volume (L)
Lung	53.0	2.10	6.08	1.11
Spleen	0.600	0.600	0.184	0.184
Liver	13.8	10.3	1.50	1.63
ACAT gut	7.50		0.836	
Adipose	0.400	10.0	0.605	30.3
Muscle	7.50	122	0.622	20.7
Heart	3.90	1.20	0.230	0.315
Brain	1.30	1.24	0.882	1.73
Kidney	9.20	3.70	1.02	0.277
Skin	5.80	40.0	0.235	1.96
Testes	0.500	2.50	0.007	0.032
Red Marrow	1.30	1.33	0.354	1.18
Yellow Marrow	0.275	2.81	0.098	3.28
Rest of body	9.01	41.5	0.529	17.6
Arterial blood	53.0	5.60	6.08	2.21
Venous blood	53.0	11.3	6.08	4.42

[a] Default values taken from the Gastroplus software 5.1.0 generic rat and human PBPK model

DMD Fast Forward. Published on July 9, 2007 as DOI: 10.1124/dmd.107.015644
This article has not been copyedited and formatted. The final version may differ from this version.

Table IV

Statistics for the predicted human pharmacokinetic parameters obtained using Method Vd1 and Method CL1 [a]

Parameter [a]	n	Average fold error (*afe*)	Root mean squared error (*rmse*)	% within 2-fold error	% within 3-fold error
Vss (L)	19	2.10	604	31.6	52.6
CL (L/h)	19	2.41	36.3	52.6	68.4
CL_R (L/h)	4	1.09	5.41	100	100
in vivo $t_{1/2}$ (h)	26	5.40	903	26.9	38.5
Vd/F (L)	23	1.38	9.33E+03	21.7	39.1
AUC (ng.h/ml)	23	5.09	7.91E+04	34.8	43.5
C_{max} (ng/ml)	23	1.39	2.94E+03	65.2	69.6
F (%)	16	1.60	31.0	62.5 [b]	-

[a] See Methods for more details on prediction of each parameter using Method Vd1 and/or Method CL1. Vss, apparent volume of distribution at steady-state; CL, total body clearance from plasma; CL_R, renal clearance from plasma; *in vivo* $t_{1/2}$, *in vivo* terminal half-life; Vd/F, volume of distribution during terminal phase after oral dosing; AUC, area under plasma concentration-time curve after oral dosing; C_{max}, peak plasma concentration after oral dosing; F, absolute oral bioavailability

[b] % within 1.5-fold error

DMD Fast Forward. Published on July 9, 2007 as DOI: 10.1124/dmd.107.015644
This article has not been copyedited and formatted. The final version may differ from this version.

Table V

Statistics for the predicted human pharmacokinetic parameters obtained using Method Vd2 and Method CL2 [a]

Parameter [a]	n	Average fold error (*afe*)	Root mean squared error (*rmse*)	% within 2-fold error	% within 3-fold error
Vss (L)	19	1.14	207	84.2	94.7
CL (L/h)	19	1.10	31.3	73.7	89.5
CL_R (L/h)	4	1.09	5.41	100	100
in vivo $t_{1/2}$ (h)	26	1.49	8.72	69.2	88.5
Vd/F (L)	23	1.32	2.10E+03	69.6	82.6
AUC (ng.h/ml)	23	1.06	6.45E+03	73.9	87.0
C_{max} (ng/ml)	23	1.31	2.01E+03	65.2	91.3
F (%)	16	1.06	15.0	81.3 [b]	-

[a] See Methods for more details on prediction of each parameter using Method Vd2 and/or Method CL2. Vss, apparent volume of distribution at steady-state; CL, total body clearance from plasma; CL_R, renal clearance from plasma; *in vivo* $t_{1/2}$, *in vivo* terminal half-life; Vd/F, volume of distribution during terminal phase after oral dosing; AUC, area under plasma concentration-time curve after oral dosing; C_{max}, peak plasma concentration after oral dosing; F, absolute oral bioavailability

[b] % within 1.5-fold error

DMD Fast Forward. Published on July 9, 2007 as DOI: 10.1124/dmd.107.015644
This article has not been copyedited and formatted. The final version may differ from this version.

Table VI

Effect of plasma protein binding and source of rat P_{tp} data on prediction accuracy of human Vss using Method Vd2 [a,b]

Parameter [b]	n	fu_p [c] correction	Source of rat P_{tp} data	Average fold error (*afe*)	Root mean squared error (*rmse*)	% within 2-fold error	% within 3-fold error
Vss (L)	19	Yes	Predicted + Experimental [d]	1.14	207	84.2	94.7
Vss (L)	19	No	Predicted + Experimental [d]	1.54	361	52.6	68.4
Vss (L)	19	Yes	Predicted [e]	1.44	377	47.4	78.9
Vss (L)	19	No	Predicted [e]	1.89	600	42.1	78.9

[a] For more details on Method Vd2, see Methods

[b] P_{tp}, tissue-to-plasma coefficient; Vss, human apparent volume of distribution at steady-state

[c] "Yes" refers to the assumption that human unbound P_{tp} is equal to rat unbound P_{tp}; "No" refers to the assumption that human P_{tp} is equal to rat P_{tp}

[d] "Predicted + Experimental ": In instances where the experimental *in vivo* rat P_{tp} was not available, the value for that particular tissue was predicted as described under Method Vd2. All experimentally determined *in vivo* rat P_{tp} are given in Table II.

[e] "Predicted": only predicted rat P_{tp} values were used for all tissue compartments. All values were predicted as described under Method Vd2.

DMD Fast Forward. Published on July 9, 2007 as DOI: 10.1124/dmd.107.015644
This article has not been copyedited and formatted. The final version may differ from this version.

Table VII

Statistics for the predicted rat pharmacokinetic parameters

Parameter [b]	Method [a]	Source of rat P_{tp} data [b]	Average fold error (*afe*)	Root mean squared error (*rmse*)	% within 2-fold error	% within 3-fold error
Vss (L)	Method Vd1	Predicted [c]	1.07	3.23	42.3	53.8
Vss (L)	Method Vd2	Predicted + Experimental [d]	1.51	2.52	73.1	88.5
Vss (L)	Method Vd2	Predicted [c]	1.10	3.10	65.4	80.8
CL (L/h)	Method CL1	-	3.59	0.468	34.6	53.8
CL (L/h)	Method CL2	-	1.23	0.311	84.6	100

[a] For more details on Method Vd1, Method Vd2, Method CL1 and Method CL2, see Methods

[b] Vss, apparent volume of distribution at steady-state; CL, total body clearance from plasma; P_{tp}, tissue-to-plasma coefficient

[c] "Predicted" : only predicted rat P_{tp} values were used for all tissue compartments.

[d] "Predicted + Experimental ": In instances where the experimental *in vivo* rat P_{tp} was not available, the value for that particular tissue compartment was predicted as described under Method Vd2. All experimentally determined *in vivo* rat P_{tp} are given in Table II

DMD Fast Forward. Published on July 9, 2007 as DOI: 10.1124/dmd.107.015644
This article has not been copyedited and formatted. The final version may differ from this version.

Table VIII

Statistics for the predicted human plasma concentrations after oral dosing

Approach [a]	n	Average fold error (*afe*)	Root mean squared error (*rmse*)	% within 1.5-fold error	% within 2-fold error	% within 3-fold error
Method Vd1/CL1	261 [b]	2.29	1.57	25.7	36.5	50.9
Method Vd2/CL2	261 [b]	1.03	1.20	43.4	60.0	74.8

[a] For details on prediction of oral plasma concentrations using Method Vd1/CL1 and Method Vd2/CL2, see Methods

[b] the total pool (n=261) of mean plasma concentrations (ug/ml) for all compounds of Table II after oral dosing.

Figure 1

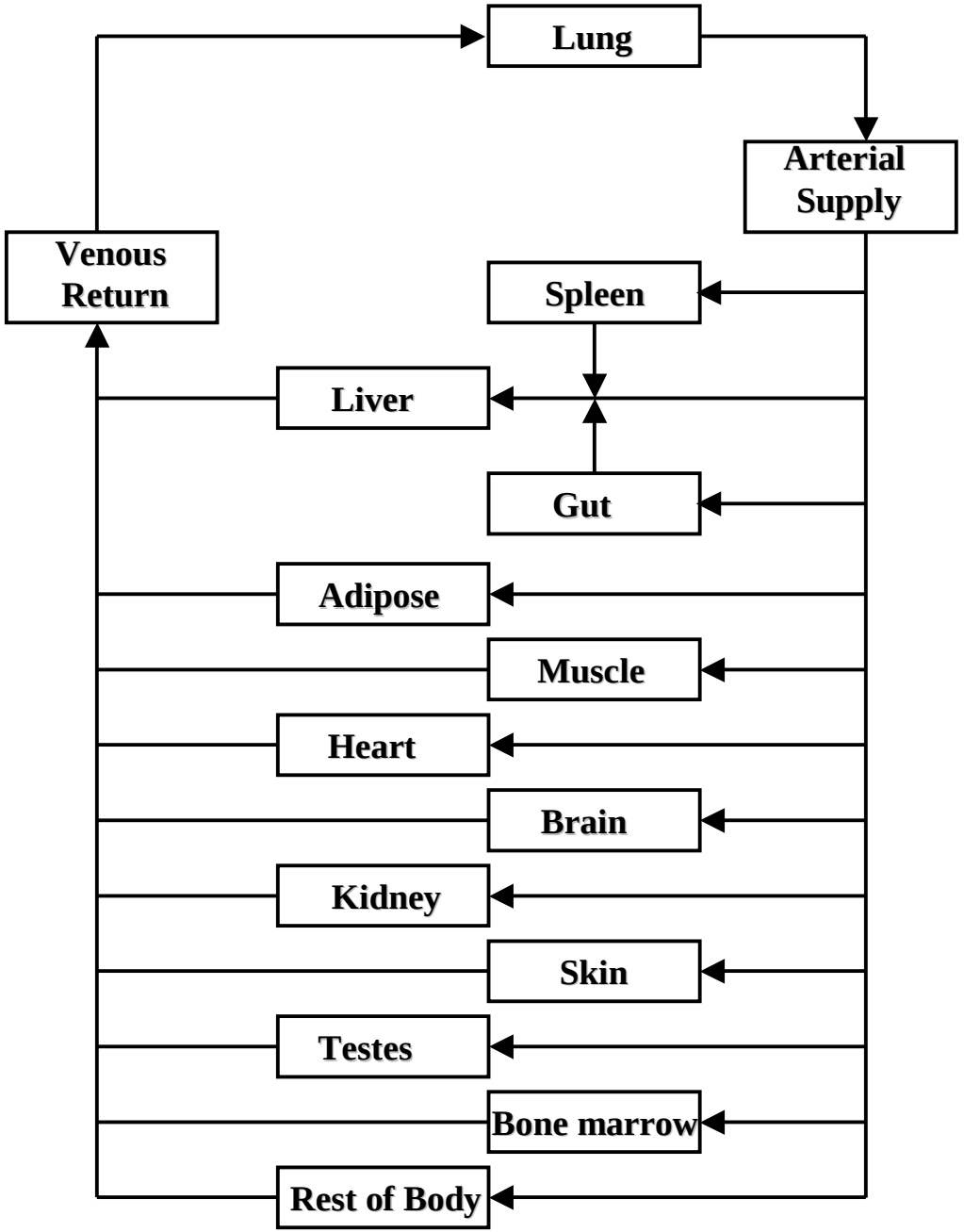

Figure 2

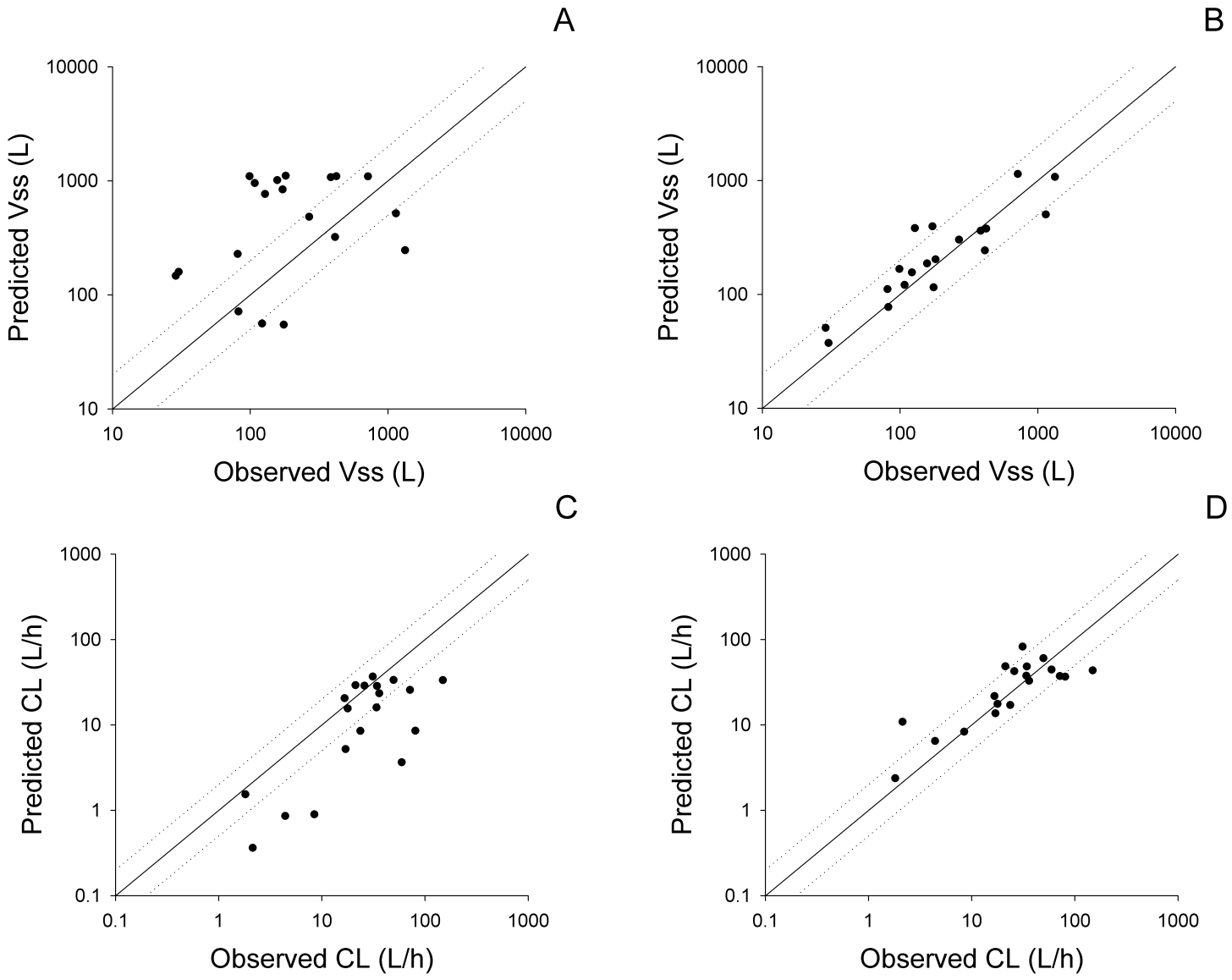

Figure 3

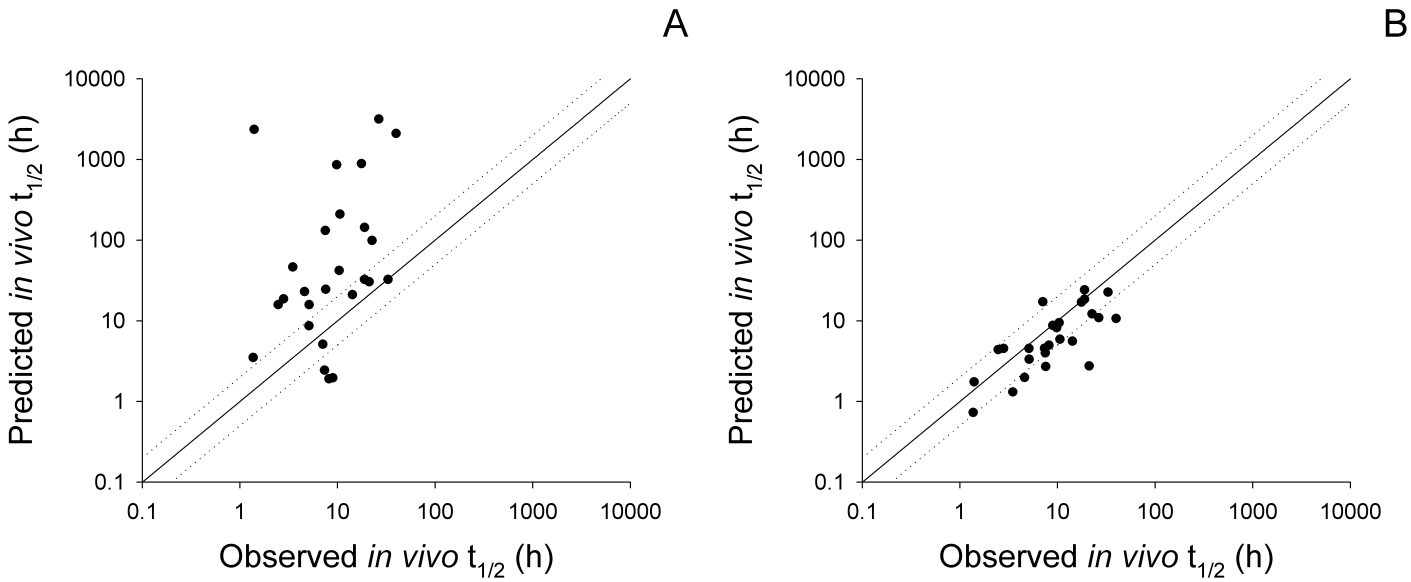

Figure 4

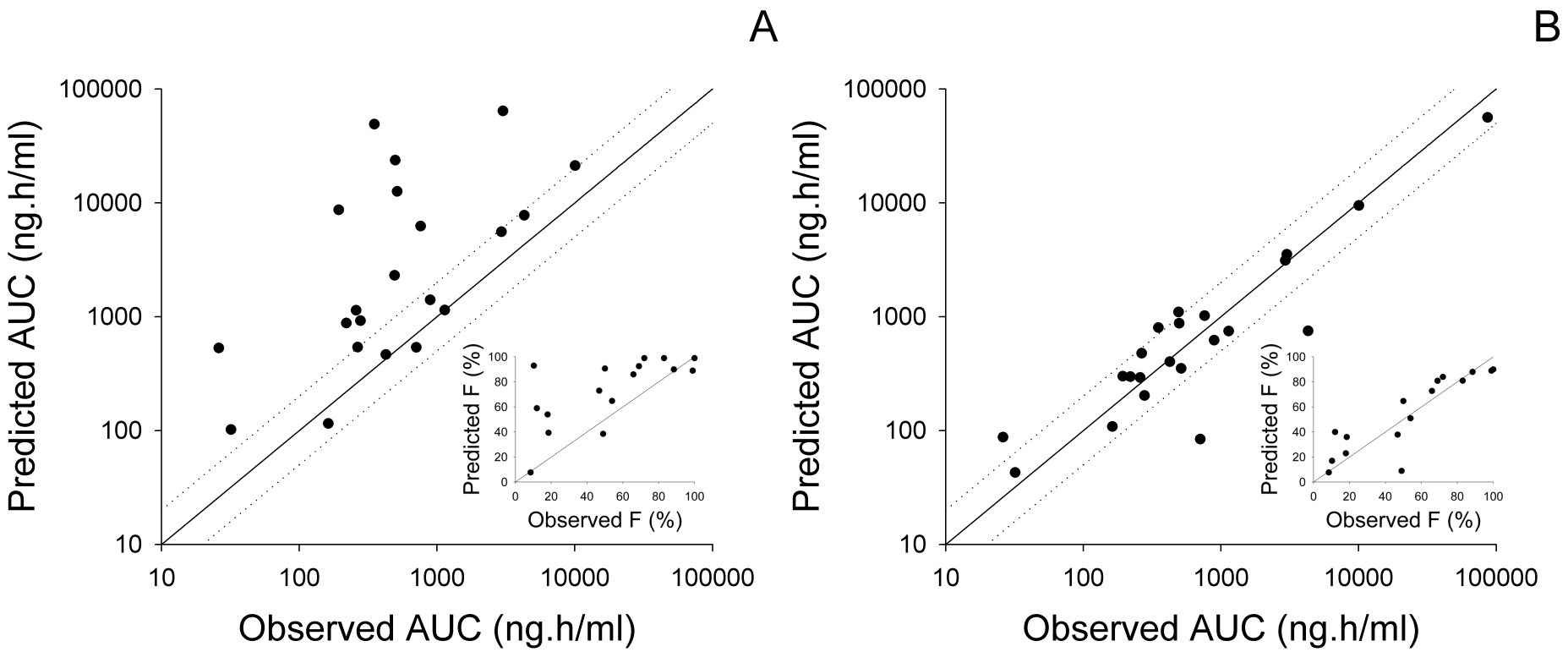

DMD Fast Forward. Published on July 9, 2007 as DOI: 10.1124/dmd.107.015644
This article has not been copyedited and formatted. The final version may differ from this version.

Figure 5

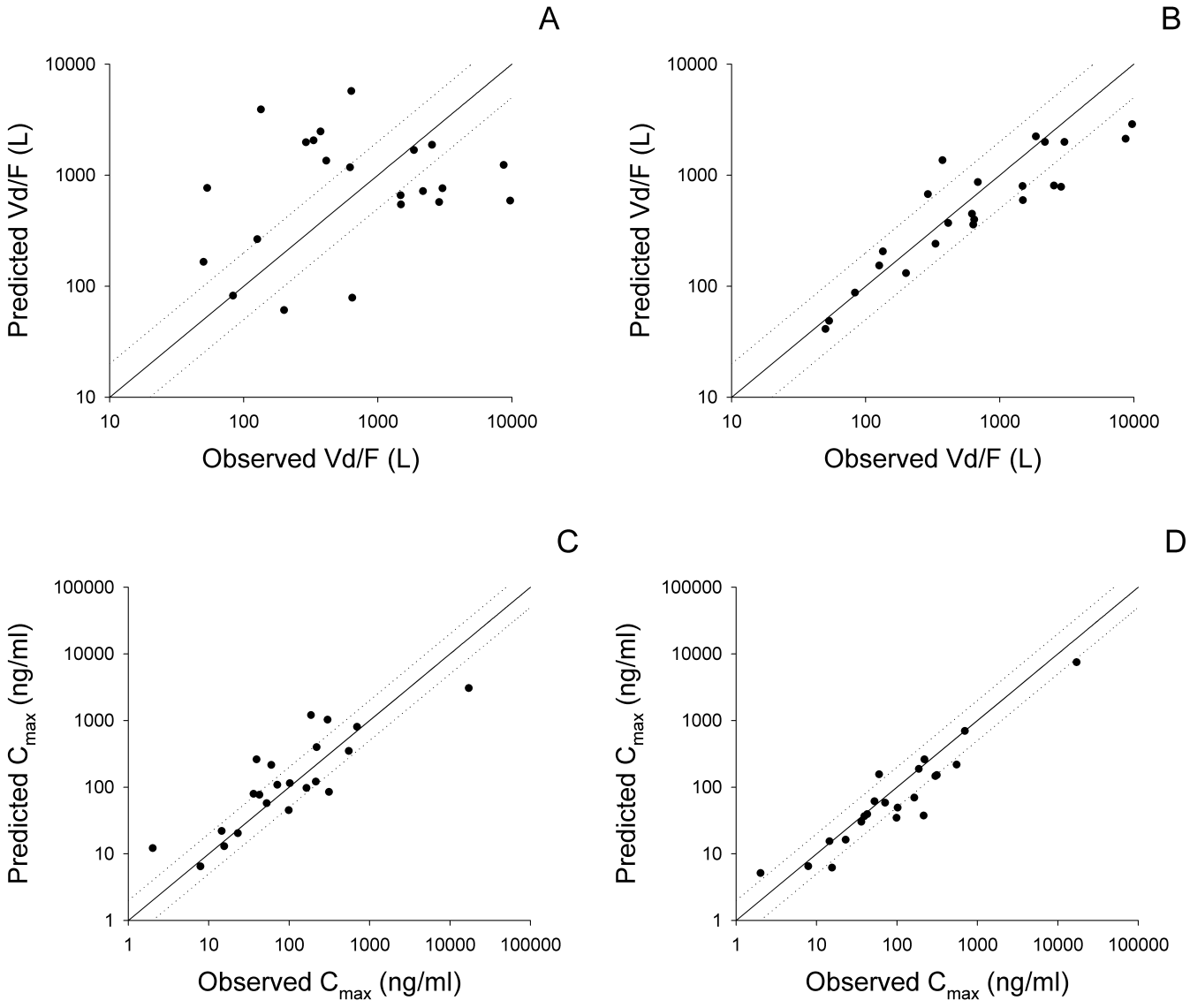

DMD Fast Forward. Published on July 9, 2007 as DOI: 10.1124/dmd.107.015644
This article has not been copyedited and formatted. The final version may differ from this version.

Figure 6